Biochimica et Biophysica Acta 1820 (2012) 1128–1140

Contents lists available at SciVerse ScienceDirect

Biochimica et Biophysica Acta

journal homepage: www.elsevier.com/locate/bbagen

Biochemical, physicochemical and molecular characterization of a genuine 2-Cys-peroxiredoxin purified from cowpea [*Vigna unguiculata* (L.) Walpers] leaves

Fredy D.A. Silva [a], Ilka M. Vasconcelos [a], Marina D.P. Lobo [a], Patrícia G. de Castro [a], Vladimir G. Magalhães [a], Cléverson D.T. de Freitas [c], Célia R.R.S. Carlini [d], Paulo M. Pinto [d], Leila M. Beltramini [e], José H.A. Filho [f], Eduardo B. Barros [g], Luciana M.R. Alencar [g], Thalles B. Grangeiro [b,*], José T.A. Oliveira [a,*]

[a] *Departamento de Bioquímica e Biologia Molecular, Universidade Federal do Ceará (UFC), CE, Brazil*
[b] *Departamento de Biologia, Universidade Federal do Ceará (UFC), CE, Brazil*
[c] *Departamento de Biologia, Universidade Federal do Piauí (UFPI), PI, Brazil*
[d] *Departamento de Biofísica, Centro de Biotecnologia, Universidade Federal do Rio Grande do Sul (UFRGS), RS, Brazil*
[e] *Instituto de Física de São Carlos (IFSC), Universidade de São Paulo (USP), SP, Brazil*
[f] *Departamento de Biologia, Universidade Regional do Rio Grande do Norte (UERN), RN, Brazil*
[g] *Departamento de Física, Universidade Federal do Ceará (UFC), CE, Brazil*

ARTICLE INFO

Article history:
Received 31 August 2011
Received in revised form 5 March 2012
Accepted 6 March 2012
Available online 17 March 2012

Keywords:
2-Cys-peroxiredoxin
Vigna unguiculata
Amino acid sequence
Circular dichroism
cDNA sequence

ABSTRACT

Background: Peroxiredoxins have diverse functions in cellular defense-signaling pathways. 2-Cys-peroxiredoxins (2-Cys-Prx) reduce H_2O_2 and alkyl-hydroperoxide. This study describes the purification and characterization of a genuine 2-Cys-Prx from *Vigna unguiculata* (Vu-2-Cys-Prx).
Methods: Vu-2-Cys-Prx was purified from leaves by ammonium sulfate fractionation, chitin affinity and ion exchange chromatography.
Results: Vu-2-Cys-Prx reduces H_2O_2 using NADPH and DTT. Vu-2-Cys-Prx is a 44 kDa (SDS-PAGE)/46 kDa (exclusion chromatography) protein that appears as a 22 kDa molecule under reducing conditions, indicating that it is a homodimer linked intermolecularly by disulfide bonds and has a pI range of 4.56–4.72; its NH_2-terminal sequence was similar to 2-Cys-Prx from *Phaseolus vulgaris* (96%) and *Populus tricocarpa* (96%). Analysis by ESI-Q-TOF MS/MS showed a molecular mass/pI of 28.622 kDa/5.18. Vu-2-Cys-Prx has 8% α-helix, 39% β-sheet, 22% of turns and 31% of unordered forms. Vu-2-Cys-Prx was heat stable, has optimal activity at pH 7.0, and prevented plasmid DNA degradation. Atomic force microscopy shows that Vu-2-Cys-Prx oligomerized in decamers which might be associated with its molecular chaperone activity that prevented denaturation of insulin and citrate synthase. Its cDNA analysis showed that the redox-active Cys^{52} residue and the amino acids Pro^{45}, Thr^{49} and Arg^{128} are conserved as in other 2-Cys-Prx.
General significance: The biochemical and molecular features of Vu-2-Cys-Prx are similar to other members of 2-Cys-Prx family. To date, only one publication reported on the purification of native 2-Cys-Prx from leaves and the subsequent analysis by N-terminal Edman sequencing, which is crucial for construction of stromal recombinant 2-Cys-Prx proteins.

1. Introduction

Superoxide ion (O^{-2}), hydrogen peroxide (H_2O_2) and hydroxyl radicals (HO^-) are generated during the aerobic metabolism of plants by mitochondria, chloroplasts and peroxisomes [1]. At physiological levels, these highly reactive oxygen species (ROS) can act as second messengers in cell signaling pathways and can ultimately lead to changes in gene expression [2]. However, under stress, ROS generation in plants can increase rapidly, and accumulation above physiological levels could damage nucleic acids, proteins and lipids [3]. As a result, ROS removal by cells is essential for survival. To prevent the toxic effects of H_2O_2, plants have developed an elaborate antioxidant enzyme system that quickly and efficiently controls the cellular level of H_2O_2. This effect is achieved by the action of enzymes,

Abbreviations: BSA, bovine serum albumin; CS, citrate synthase; CBD, chitin-binding domain; 2-Cys-Prx, 2-Cys-Peroxiredoxin; Vu-2-Cys-Prx, *Vigna unguiculata* 2-Cys-peroxiredoxin; CD, circular dichroism; H_2O_2, hydrogen peroxide; IPG buffer, ampholyte-containing buffer concentrate; IPG strips, Immobiline™ DryStrip gels for isoelectric focusing of proteins; DTT, Dithiothreitol; ESI-Q-TOF MS/MS, electrospray ionization quadrupole time-of-flight; NADPH, nicotinamide adenine dinucleotide phosphate

* Corresponding authors. Depto de Bioquímica e Biologia Molecular, Universidade Federal do Ceara, CE, Laboratório de Proteínas Vegetais de Defesa, Av. Mister Hull, P.O. Box: 60451 Fortaleza, CE, Brazil. Tel.: +55 85 33669823; fax: +55 85 33669789.
E-mail addresses: jtaolive@ufc.br (J.T.A. Oliveira), tbgrangeiro@gmail.com (T.B. Grangeiro).

0304-4165 © 2012 Elsevier B.V. Open access under the Elsevier OA license.
doi:10.1016/j.bbagen.2012.03.003

including catalase [4], ascorbate peroxidase [5] and peroxiredoxins (Prxs) [6]. 2-Cys-Prxs belong to the plant multigenic family of thiol peroxidases, which are widely distributed in all kingdoms from bacteria to mammals [7]. They have been divided into two subgroups, which are designated typical and atypical and are both characterized by the presence of two cysteine residues, which are essential for enzymatic activity [8–11]. Typical 2-Cys-Prxs are dimeric proteins present in chloroplasts, where they act against the oxidative damage of the photosynthetic apparatus [12–14]. The reaction mechanism of typical 2-Cys-Prxs is highly conserved. A cysteine residue of one chain, the peroxidatic cysteine (C_P), reduces H_2O_2 or other peroxides and becomes transiently oxidized to Cys-sulfenic acid, which is reduced by a second cysteine residue near the C-terminal end of the other subunit of the dimer, the resolving cysteine (C_R). The reaction yields water or alcohol and forms an intermolecular disulfide bridge. Subsequently, the free thiol forms of C_P and C_R are usually regenerated by a thioredoxin-like molecule to complete the catalytic cycle [15,16]. Generally native atypical 2-Cys-Prxs are dimeric proteins with monomers linked together by hydrophobic interaction and they differ from typical 2-Cys-Prxs because the catalytic mechanism involves intramolecular disulfide bond generation [15–17]. In both classes of 2-Cys-Prx, the disulfide bonds formed are reduced *in vitro* for a new catalytic cycle by the action of the electron donors thioredoxin [18], cyclophilin [19] and glutaredoxin [20], which all use NADPH as a source of reducing power. However, when at high concentrations of H_2O_2 the Cys-sulfenic acid is overoxidized to Cys-sulfinic acid, an additional system, the sulfiredoxin system [21], reduces 2-Cys-Prx to the free thiol form. Recently, it was reported that NADPH thioredoxin reductase C is the most relevant pathway for the reduction of chloroplast 2-Cys-Prxs *in vivo* [22,23] and it might also act as an electron donor to Prxs in the cytosol, mitochondria, and plastids of the symbiotic nodules of the legume *Lotus japonicus* [24]. The biochemical and physicochemical characteristics of various 2-Cys-Prxs of plant origin have been studied over the last 10 years, such as those of *Arabidopsis thaliana*, *Brassica campestris*, *Hordeum vulgare*, *Phaseolus vulgaris* and *Pisum sativum* [25,8,19,26]. However, to date, only one publication was reported on the purification of native 2-Cys-Prx from leaves and the subsequent analysis by N-terminal Edman sequencing [27], which is crucial for construction of stromal recombinant 2-Cys-Prx proteins. In this study we describe the purification of an authentic 2-Cys-Prx from cowpea leaves that may play a pivotal role in the protection of plant chloroplasts from photo-oxidative stress, and further present its biochemical, structural and molecular properties.

2. Materials and methods

2.1. Materials

Acrylamide, bis-acrylamide, sodium dodecyl sulfate, NADPH, DTT, thioredoxin, thioredoxin reductase and chitin were purchased from Sigma, St. Louis, USA. IPG buffer and IPG strips, both at pH range of 4–7, were from GE Lifesciences (Piscataway, NJ, USA). Superose 12 HR 10/30 and Resource-Q were purchased from GE Healthcare, NJ, USA. Plasmid pGEM-T Easy was purchased from Promega (Madison, WI, USA). The *Escherichia coli* general cloning strain TOP10F′ was purchased from Invitrogen (Carlsbad, CA, USA). All other chemicals were of analytical grade and were purchased from diverse companies.

2.2. Plant and growth conditions

Cowpea [*Vigna unguiculata* (L.) Walp.] seeds of the Brazilian genotype TE-97411-1F were a generous gift from Dr. Francisco R. Freire-Filho of Empresa Brasileira de Pesquisas Agropecuárias (EMBRAPA), Meio Norte, Piauí, Brazil. The seeds were surface sterilized with sodium hypochlorite (0.1% active chlorine) for 1 min and rinsed thoroughly with distilled water. They were soaked in distilled water for 20 min and planted in autoclaved (121 °C, 9.8×10^4 Pa, 30 min) germination paper (Germitest ®). Three days later, six germinated seedlings were transferred to a 1 L plastic pot containing autoclaved river sand previously washed with tap water and distilled water. The pots were kept in a greenhouse inside a four-legged aluminum framework covered with a transparent nylon net. The plantlets were watered daily with distilled water until the sixth day after planting and were subsequently watered with Hoagland and Arnon's nutrient solution diluted 1:10 (v/v) in distilled water [28] with a fixed volume of 100 mL per pot. The plants were exposed to natural light [ca. 700 μmol m^{-2} s^{-1} of photosynthetically active radiation (PAR) at the plant canopy] with a photoperiod of approximately 12 h light/12 h dark, with temperatures varying from 27.0 ± 0.8 °C (night) to 31.0 ± 3.0 °C (day) and relative humidity of 79.8 ± 10.9%. Fifteen days after planting, the healthy plants were selected, and their primary and secondary leaves were collected, washed with distilled water, and stored at −80 °C until used.

2.3. Enzyme extract

Frozen cowpea leaves (1390 g) were ground in liquid nitrogen and the soluble proteins extracted with SA buffer (50 mM sodium acetate at pH 5.2, containing 500 mM NaCl, 30 mM ascorbic acid, 3 mM EDTA, and 1% polyvinylpyrrolidone) in the proportion of 1:2 (w/v). The resulting suspension was stirred for 30 min, filtered through one layer of muslin cloth and centrifuged at 12,500 *g* for 30 min at 4 °C. The supernatant was dialyzed against the extraction buffer and centrifuged, and the protein extract (3560 mL) obtained was used for purification of the enzyme.

2.4. Protein purification

The protein extract (3550 mL) was fractionated 30–60% saturation with ammonium sulfate, and the precipitated proteins were recovered by centrifugation at 10,000×*g* for 30 min at 4 °C. This precipitate was resuspended and dialyzed against the SA buffer, and 214.45 mL of the 30–60% fraction obtained (F30–60) was applied on a chitin column (3×28 cm; Sigma Aldrich) previously equilibrated with the same buffer. The column was first washed with the equilibrium buffer at a flow rate of 1 mL min^{-1}, 25 °C, and the chitin-bound proteins (CCII) were eluted with 100 mM acetic acid. Fractions of 2 mL were collected and read at 280 nm. The fractions that contained 2-Cys-Prx activity were pooled and dialyzed against 50 mM sodium acetate buffer (pH 5.2), and 40.0 mL of the CCII were loaded on a Resource-Q column (1 mL; GE Healthcare) equilibrated with the same buffer. The unbound proteins were eluted with the equilibration buffer, and the bound proteins were eluted in a step-wise fashion with 100, 200, 300, 400, and 10^3 mM NaCl, prepared in the acetate buffer, at a 1 mL min^{-1} flow rate. Fractions of 2 mL were collected and read at 280 nm, and the 2-Cys-Prx activity was assayed.

2.5. Protein concentration

The protein concentration was determined according to Bradford [29] using BSA as a standard. Absorbance at 280 nm was also used to monitor protein elution profiles during chromatography.

2.6. 2-Cys-Prx activity

The reaction mixture (300 μL) contained 50 mM potassium phosphate buffer pH 7.0, 150×10^{-3} mM NADPH, 5×10^{-3} mM thioredoxin, 1.6×10^{-3} mM thioredoxin reductase and different aliquots of the crude extract, protein fractions, and purified cowpea 2-Cys-Prx (Vu-2-Cys-Prx). Oxidation of NADPH at 30 °C was initiated by adding 50×10^{-3} mM H_2O_2 and was monitored at 340 nm in a Novaspec II spectrophotometer (Phamarcia LKB) for 2 min [9]. The rates of

NADPH oxidation in the absence of Prx were also recorded and subtracted from the experimental rates. NADPH oxidation was monitored as the decrease in A_{340} in a 300 μL reaction mixture. The capacity of Vu-2-Cys-Prx to use DTT as reducing power was determined by the rate of DTT oxidation [30]. The following were incubated at 37 °C in a 1.0 mL reaction volume: 68×10^{-3} mM of Vu-2-Cys-Prx (apparent native molecular mass of 44 kDa), 100 mM sodium phosphate buffer pH 7.0, 1 mM EDTA and 150×10^{-3} mM H_2O_2. The reaction was started by addition of 1.0 mM DTT, and the rate of DTT oxidation was monitored at 310 nm. Activity was calculated on the basis of the absorption coefficient of oxidized DTT ($\varepsilon = 110\ M^{-1}\ cm^{-1}$).

2.7. Molecular weight determination by SDS-PAGE and gel filtration

The apparent molecular weight and the subunit constituents of Vu-2-Cys-Prx were determined by denaturing electrophoresis (SDS-PAGE) using 12.5% polyacrylamide gels (8.5×8.0 cm) as described by Laemmli [31]. Samples were heated at 100 °C for 5 min in the presence or absence of 5% β-mercaptoethanol and were centrifuged (12,500 *g*, 10 min, 4 °C) before electrophoresis. Samples (5 μg protein) were loaded on the gel and the analysis was performed at 20 mA for approximately 90 min. Protein bands were visualized as described by Candiano et al. [32], and the molecular weight was determined on the basis of protein markers analyzed concomitantly. The native molecular weight of the protein was also determined using a superose-12 HR column (1×30 cm; GE Healthcare) by applying 100 μL of a solution containing 60 μg protein dissolved (1.36×10^{-3} mM) in 50 mM sodium acetate buffer at pH 5.2. The column was equilibrated, and the protein was eluted at a 0.3 mL min^{-1} flow rate with the sodium acetate buffer. The elution profile was monitored at a wavelength of 280 nm. Alcohol dehydrogenase (150 kDa), bovine serum albumin (66 kDa), egg albumin (45 kDa), trypsinogen (24 kDa) and cytochrome c (12.4 kDa) were used as standards.

2.8. Establishment of the optimal pH of activity

The assay based on NADPH oxidation was conducted as previously described [9]. A solution of 68×10^{-3} mM Vu-2-Cys-Prx was used. The reaction mixture was buffered with two different solutions for each pH assayed, as following: pH 3.0, 50 mM sodium citrate and 50 mM glycine-HCl; pH 4.0 and 5.0, 50 mM sodium acetate and 50 mM sodium citrate, respectively; pH 6.0, 50 mM sodium acetate and 50 mM sodium phosphate; pH 7.0 and 8.0, 50 mM sodium phosphate and 50 mM Tris–HCl, respectively; pH 9.0, 50 mM Tris–HCl and 50 mM sodium borate. ANOVA followed by Tukey's test (Assistat Program) [33] was carried out with the data obtained to check for statistic differences (Fig. 3C).

2.9. Two-dimensional gel electrophoresis

DTT-treated and DTT-untreated Vu-2-Cys-Prx (6 μg protein) samples were mixed with the rehydration buffer (8 M urea, 1 M thiourea, 2% CHAPS, 10% glycerol, 2% IPG buffer pH 4–7 and 0.002% bromophenol blue) to a final volume of 250 μL [34]. These samples were incubated with 13-cm IPG strips in the pH range of 4–7 and allowed to rehydrate for 15 h (overnight). The first-dimension isoelectric focusing (IEF) was performed in a Multiphor III apparatus (GE Lifesciences) at 200 V for 30 min, 500 V for 30 min, 1000 V for 1 h, 2500 V for 1 h and 3500 V for 5 h, for a total of 8000 V/h. After IEF, the strip was equilibrated for 15 min in equilibration buffer containing 2.5% DTT (for samples treated with DTT) and iodoacetamide and transferred to the top of a vertical polyacrylamide gel (16×18×0.1 cm). The second dimension SDS-PAGE in 12.5% gels was performed according to Görg et al. [35] with minor modifications at 300 V, 30 mA for approximately 6 h using a Hoefer SE 600 Series electrophoresis unit (GE Healthcare). The protein spots were revealed with colloidal Coomassie G-250 as previously described [32], and the gel was scanned at 600 dpi with an ImageScanner II (GE Healthcare Lifesciences).

2.10. NH_2-terminal sequencing

NH_2-terminal sequencing was determined on a Shimadzu PPSQ-10 Automated Protein Sequencer performing Edman degradation. Phenylthiohydantoin amino acids were detected at 269 nm after separation on a reversed-phase C_{18} column (4.6×2.5 mm) under isocratic conditions according to the manufacturer's instructions. Searches for sequence similarity were performed with the BLASTp program [36].

2.11. Mass spectrometry analysis

The mass spectrum of Vu-2-Cys-Prx was acquired by an electrospray ionization (ESI) quadrupole time-of-flight (Q-TOF) Micro™ mass spectrometer coupled with a nanoACQUITY® UltraPerformance liquid chromatography system (LC) (Waters, Milford, US). A nanoflow ESI source was used with a Lockspray™ dual electrospray ion source (Waters). The spots of the 2D gel were excised and destained with 100 μL of 25 mM NH_4HCO_3 in 50% acetonitrile (ACN) and 100% ACN for 10 min and dried under a vacuum for 30 min. The dried gel pieces were incubated with trypsin (10 ng μL^{-1} in 50 mM NH_4HCO_3) at 37 °C in a water bath overnight [37]. The peptides were extracted for 30 min with 50% ACN/5% trifluoroacetic acid and were concentrated to a final volume of 20 μL. An aliquot of 10 μL was added to the MALDI plate, and matrix crystallization occurred at room temperature prior to mass spectrometer analysis. The mass spectra were obtained in interactive mode, in which all of the samples were automatically analyzed in the MS reflector mode, and the two most intensive peaks were subjected to further MS/MS analysis. The LC and ESI conditions consisted of a flow of 600 nL min^{-1}, a nanoflow capillary voltage of 3.5 kV, a block temperature of 100 °C, and a cone voltage of 50 V. The results were analyzed using the GPS Explorer™ (Applied Biosystems), for which the MS and MS/MS data were processed and submitted jointly to the MASCOT search program (Matrix Science, London, UK). Searches were conducted considering a maximum of one missed cleavage, the carbamidomethylation of cysteine, the possible oxidation of methionine, a peptide tolerance of 0.2 Da, and a MS/MS tolerance of 0.2 Da. The data obtained from the spectra were filtered by a signal to noise ratio of 20 for the MS data and 10 for MS/MS and were submitted for peptide mass homology and amino acid sequence comparison searches at the NCBI (National Center for Biotechnology Information: www.ncbi.nlm.nih.gov/NCBInr) protein database, restricted to Viridiplantae (Green Plants).

2.12. Far-UV circular dichroism (CD) spectroscopy

CD spectra measurements were performed on a JASCO J-715 spectropolarimeter (Jasco Instruments, Tokyo, Japan) under an N_2 atmosphere at 25 °C. Native Vu-2-Cys-Prx (90×10^{-3} μM) was dissolved in 25 mM phosphate buffered saline at pH 7.0 containing 1.0 mM EDTA (PBE) and was transferred to a 0.1 cm path length cylindrical quartz cuvette. Eight scans were performed with a scan rate of 20 nm min^{-1} and a 4 s response time. CD spectra were measured from 190–195 to 250 nm. The contributions of the secondary structural elements of Vu-2-Cys-Prx were determined by CD spectrum deconvolution analyses using the basis reference protein set SMP56 of the CDPro software [38] using three methods, CONTIN/LL, SELCON 3, and CDSSTR. The most consistent results were produced by CONTIN/LL. CD spectroscopy was also employed to assess Vu-2-Cys-Prx thermal stability. The protein sample (90×10^{-3} mM in PBE) was heated gradually in 10 °C increments from 25 to 95 °C in a TC-100 circulating water bath (Jasco). The samples were maintained

at each temperature for 30 min, and spectra were recorded from 195 to 250 nm.

2.13. Fluorescence experiments and pH stability (intrinsic and extrinsic probes)

Fluorescence emission measurements were performed with a spectrofluorimeter (ISS, IL, USA; model ISS K2) equipped with a refrigerated circulator (Neslab RTE-210). The excitation and emission monochromators were set at 2 nm and 1 nm slit widths, respectively. All of the fluorescence measurements were performed in rectangular quartz cuvettes (1 cm path length). Reference spectra were recorded and subtracted after each measurement.

The intrinsic fluorescence spectrum of a Vu-2-Cys-Prx sample (90×10^{-3} mM) in PBE was measured after excitation at 280 and 295 nm (tyrosine and tryptophan amino acid excitations, respectively), and emission spectra were monitored from 280 to 460 nm. Fluorescent dye binding experiments using 13.4×10^{-3} mM 1-anilino-8-naphthalene-sulfonic acid (ANS) were performed to probe extrinsic dynamic changes in the protein and the exposure of hydrophobic regions [39]. Changes in surface hydrophobicity as a function of pH were measured at a fixed concentration of ANS (13.4 μM), which was mixed with Vu-2-Cys-Prx solution (90×10^{-3} mM) prepared in different buffers (25 mM glycine-HCl at pH 3.0; 25 mM PBE at pH 7.0; and 25 mM Tris–HCl at pH 9.0). The excitation wavelength was set at 380 nm, and the emission spectrum was monitored from 380 nm to 650 nm at 22 °C.

2.14. Antioxidant assay

The antioxidant activity of Vu-2-Cys-Prx was assessed *in vitro* [40] on the basis of the protection of plasmid DNA exposed to radicals generated by the presence of 3 mM $FeCl_3$ and 4 mM DTT (oxidant system). The plasmid DNA pGEM T-easy (Promega ®) was incubated at 37 °C for 2 h in the absence and presence of the oxidant system with Vu-2-Cys-Prx or BSA, both at 23×10^{-3}, 45×10^{-3}, and 90×10^{-3} mM concentrations in 50 mM phosphate buffer at pH 7.0. Protection of plasmid DNA against oxidation was assessed by confirming its integrity after electrophoresis in 1% agarose gel and by incubation in ethidium bromide.

2.15. Assay of molecular chaperone activity

Chaperone activity of Vu-2-Cys-Prx (10^{-3} mM) was measured on Citrate synthase (CS, 10^{-3} mM), and insulin (5×10^{-3} mM), using DTT (10 mM) as reducing agent, dissolved in 50 mM phosphate sodium buffer pH 7.0 in a 1.0 mL reaction mixture. Absorbances were monitored in a spectrophotometer (Ultospec III, Pharmacia LKB) and increased turbidity due to thermal aggregation, at 45 °C, of CS and the chemical aggregation of insulin induced by DTT was monitored at 360 nm [41]. BSA (5×10^{-3} mM) was incubated with both CS and insulin as controls.

2.16. Oligomerization assay

The possible oligomerization states of Vu-2-Cys-Prx were evaluated by subjecting the protein to various treatments: dissolving in 50 mM PBE buffer at pH 7.0 in the presence of 100 mM DTT; in the presence of 5×10^{-3} mM thioredoxin, 1.6×10^{-3} mM thioredoxin reductase, 150×10^{-3} mM NADPH and 100 mM H_2O_2; with 1.5×10^{3} mM NaCl; heating for 20 min; dissolved in 50 mM Na-citrate buffer at pH 2.0; and in 50 mM Na-borate buffer at pH 11.0. Untreated Vu-2-Cys-Prx was used as control. The oligomerization states of Vu-2-Cys-Prx were evaluated by polyacrylamide gel electrophoresis (10%) in the presence of SDS [31].

2.17. Atomic force microscopy (AFM)

For the analysis of atomic force microscopy, purified Vu-2-Cys-Prx was lyophilized and the powder reconstituted in 1 mgP/mL of Vu-2-Cys-Prx in 50 mM, sodium phosphate buffer, pH 7.0, centrifuged at 12,000 *g* for 15 min at 4 °C and treated with 100 mM DTT for 10 h. Then aliquots of 20 μL of the protein solution treated were directly applied to a freshly cleaved mica surface previously treated with 0.1% poly-L-lysine and incubated at room temperature for 30 min. After incubation the mica surface was washed several times with Milli-Q grade water to remove proteins not adsorbed and incubated in a dessicator for 2 h. The images were generated by a Multimode Nanoscope IIIa equipment (Bruker, Santa Barbara, CA) using intermittent (or tapping) mode scan using a TESP7 tip (Bruker), with nominal spring constant of 20–80 N/m. The measurements were performed in air with a scan rate of 0.5 Hz. The images presented were obtained in phase mode and are zoomed up areas from original images of 500 nm of lateral size with a resolution of 512 per 512 lines. The relative humidity during the data acquisition was of about 44%.

2.18. RNA purification

Total RNA was extracted from *V. unguiculata* leaves (100 mg) using Trizol reagent (Invitrogen) according to the manufacturer's instructions. The integrity of the RNA samples dissolved in 0.1% diethylpyrocarbonate-treated water was confirmed by 1% agarose gel electrophoresis, and the yield was estimated by measuring the absorbance at 260 nm [42].

2.19. cDNA synthesis, PCR amplification and cloning

Prior to cDNA synthesis, total RNA was treated with RQ1 RNase-free DNase I (Promega) at 37 °C for 30 min (1 unit of DNase I for each μg of RNA) and clean-up was performed using the RNeasy Mini Kit (Qiagen, Hilden, Germany). Treated RNA (recovered in 30 μL of nuclease free water) was used for cDNA synthesis with oligo$(dT)_{18}$ (Fermentas Life Sciences, Ontario, Canada) and the ImProm-II Reverse Transcription System (Promega) according to the protocol supplied by the manufacturer. The first-strand cDNA products were amplified by a polymerase chain reaction using two degenerate oligonucleotide primers, 5′-CCGCACGTGGCYTCBDSYGARYTWCCRYTRGTTGG-3′ (forward) and 5′-CCGCCTAGGMAYMGCWGCWGMRAAGTASTCTTTGCTA-3′ (reverse). Sites for restriction endonucleases were incorporated in the forward (*Pml*I) and reverse (*Avr*II) primers (underlined) to allow further manipulation of amplified fragments. The design of these primers was based on a multiple alignment of cDNA sequences (retrieved from the GenBank database) encoding 2-Cys-Prxs from *Glycine max* (AK286688, BT092170 and BT096780), *P. sativum* (AJ315851) and *P. vulgaris* (AJ288895). The oligonucleotides were designed to amplify the cDNA segment that encodes only the mature protein without the signal peptide. Amplifications were carried out in a final volume of 10 μL containing first-strand cDNA (1 μg), 1× GoTaq reaction buffer (Promega), 1.5 mM $MgCl_2$, 0.2 mM of each dNTP, 5×10^{-4} mM of each primer, and 1.25 U of GoTaq DNA Polymerase (Promega). Reactions were performed in the Mastercycler gradient thermocycler (Eppendorf, Hamburg, Germany) using the following cycling parameters: an initial denaturation step (2 min at 95 °C) followed by 35 cycles of 30 s at 95 °C, 1 min at 55 °C, and 1 min at 72 °C. After the last cycle, the reactions were further incubated for 10 min at 72 °C. The amplification of a DNA band with the expected size was confirmed by analyzing a 5 μL aliquot of the PCR reactions by 1% agarose gel electrophoresis. An aliquot of the remaining reaction (1.5 μL) was ligated into the pGEM-T Easy vector using T4 DNA Ligase. Products from the ligation reaction were introduced in *E. coli* TOP10F′ by electroporation and the transformants were selected on LB agar containing 100 μg mL^{-1} carbenicillin. Plasmid DNA was

isolated from antibiotic-resistant colonies using the alkaline lysis method [42], and the presence of the inserts was confirmed by applying restriction digestion with the appropriate endonucleases.

2.20. DNA sequencing

DNA sequencing of cloned PCR products was performed with the DYEnamic ET Dye terminator cycle sequencing kit (GE Healthcare, Buckinghamshire, UK) following the protocol supplied by the manufacturer. Reactions were carried out in 10 μL total volume containing 360 ng of the purified plasmids, and both strands were sequenced using the universal primers M13(−40) forward (5′-GTTTTCCCAGTCACGACGTTGTA-3′) and M13(−46) reverse (5′-GAGCGGATAACAATTTCACACAGG-3′). Prior to capillary electrophoresis, 10 μL agarose was added (0.06% final concentration) to the sequencing products resuspended in 10 μL 70% formamide/1 mM EDTA, as previously suggested [43,44]. Sequencing reactions were analyzed in a MegaBACE 1000 automatic sequencer (GE Healthcare). The parameters for the sequencing runs were injection at 3 kV for 50 s and electrophoresis at 6 kV for 180 min. Automated base-calling was performed using Cimarron 3.12 software, and the electropherograms were visualized with Sequence Analyzer v3.0 (Amersham Biosciences, Sunnyvale, CA, USA). The base sequences were then deduced by inspection of each processed data trace, and the complete sequences were assembled using the Cap3 software [45]. The cDNA sequence encoding the cowpea 2-Cys-Prx (Vu-2-Cys-Prx) was deposited in GenBank (accession number JF438998). Searches for homologous sequences deposited on the NCBI database were performed using the BLAST program [36]. Multiple sequence alignments were generated and manually edited using the programs ClustalW [46] and BioEdit [47], respectively. The presence of conserved domains and other conserved structural features, such as binding and catalytic sites, were identified by similarity searches on the Conserved Domain Database, CDD (www.ncbi.nlm.nih.gov/Structure/cdd/cdd.shtml).

3. Results and discussion

3.1. Purification and biochemical properties of Vu-2-Cys-Prx

A 2-Cys-Prx from cowpea (*V. unguiculata*) leaves, named Vu-2-Cys-Prx, was purified to homogeneity by fractionation of the dialyzed protein extract by ammonium sulfate precipitation followed by chitin chromatography and ion exchange chromatography on a Resource Q® column. After ammonium sulfate fractionation at 30–60% saturation, the specific activity was 2.2 times higher with a 51.7% yield of the enzyme activity (Table 1). The 30–60% fraction was loaded on a chitin column and two fractions, CCI, eluted with 50 mM sodium acetate at pH 5.2 (equilibrium buffer), and CCII, eluted with 100 mM acetic acid, were recovered (Fig. 1A). The retained fraction (CCII) showed 2-Cys-Prx activity but not chitinolytic activity on colloidal chitin as a substrate (data not shown). In the literature, a chitin-binding domain (CBD) is not described for 2-Cys-Prx. This domain is also absent in the putative sequence of Vu-2-Cys-Prx (Fig. 10), indicating that the interaction with chitin might not be through this mechanism. For example, it was recently shown that peroxidases from various plant species such as wheat (*Triticum aestivum*), rice (*Oryza sativa*), corn (*Zea mays*), radish (*Raphanus sativus*), Arabidopsis (*A. thaliana*), potato (*Solanum tuberosum*), cucumber (*Cucumis pepo*), peanut (*Arachis hypogaea*), pea (*P. sativum*) and others belonging to different families bind to chitin through other mechanisms besides the classical CBD [48]. The vicilins (7S storage proteins) from cowpea also bind to chitin, to regenerated chitin (fully acetylated chitin) and to chitosan (deacetylated chitin), but these interactions are not through CBD because cowpea vicilins do not share this sequence with CBD-containing defense proteins, such as the wheat germ agglutinin and a chitinase isolated from cowpea seeds [49]. Nevertheless, at this step, using chitin chromatography, the enzyme was purified 17.6 times with a 26.3% yield (Table 1). CCII was subjected to ion-exchange chromatography on a Resource Q® column (Fig. 1B). The RQIV peak was eluted with 300 mM NaCl in 50 mM sodium acetate buffer at pH 5.2 and retained all of the extracted 2-Cys-Prx activity of cowpea leaves. At this final step, the enzyme was purified 129 times with a low yield of 15.8% and a specific activity of 1.071 UA/mgP (Table 1). The purification protocol used in our study allowed the recovery of 2.1 mg of Vu-2-Cys-Prx starting from 1725.3 mg protein from cowpea leaves (Table 1) or 0.6 mg of Vu-2-Cys-Prx per liter of crude extract. This yield is relatively low compared with recombinant systems, in which between 7 and 30 mg of recombinant protein per liter of culture were obtained [50]. SDS-PAGE of RQ-IV (Vu-2-Cys-Prx) in the absence of β-mercaptoethanol showed the presence of a single protein band of 44 kDa (Fig. 1B, insert lane 4) free of contaminants. Under reducing conditions by treatment of Vu-2-Cys-Prx with 0.5% β-mercaptoethanol, only one protein band of approximately 22 kDa was visualized by SDS-PAGE (Fig. 1B, insert lane 5), which was consistent with the results observed for 2-Cys-Prxs of *H. vulgare* (26 kDa), *A. thaliana* (29.1 and 29.6 kDa), *P. vulgaris* (22 kDa), and *P. sativum* (22 kDa) [8,25,19]. The 2-Cys-Prxs are dimeric enzymes that form an intermolecular disulfide bridge between two head-to-tail identical subunits [51]. Therefore, the protein bands of 44 kDa and 22 kDa observed by SDS-PAGE in the absence and presence of β-mercaptoethanol, respectively, might correspond to the monomeric and dimeric forms of Vu-2-Cys-Prx. The dimeric form (44 kDa) probably results from intermolecular disulfide bridges established between the 22 kDa monomers revealed after treatment with β-mercaptoethanol [9,19]. Typical 2-Cys-Prxs contain two highly conserved Cys residues in their NH_2- and COOH-terminal regions, respectively, which form dimers during H_2O_2 catalysis [15].

The molecular mass was also assessed by size-exclusion chromatography on a Superose 12 HR column. The dimer dissolved in the equilibrium buffer (50 mM sodium acetate buffer at pH 5.2) demonstrated a molecular mass of 46 kDa (Fig. 2). This value is similar to the mass obtained by SDS-PAGE in the absence of the reducing agent β-mercaptoethanol. The recombinant 2-Cys-Prx dimers of *P. sativum*, *P. vulgaris* and *A. thaliana* have a molecular mass range of 44 to 58 kDa [19,25,8]. The dimer constitutes the minimal catalytic unit of the enzyme but can rearrange into decamers and oligomeric complexes depending on the ionic strength of the environment and the redox state of the dimers [9,26].

Table 1
Purification scheme of leaf Vu-2-Cys-Prx.

Steps	Total activity[a] (U*)	Total protein (mg)	Specific activity ($U.mg^{-1} \times 10^3$)	Purification (x)	Yield (%)
Leaf extract	14.25	1725.3	8.3	1.0	100
F30–60	7.50	410.0	18.3	2.2	51.7
CCII[b]	3.75	25.6	146.5	17.6	26.3
RQIV[c]	2.25	2.1	1071.4	129.1	15.8

[a] The reaction mixture (300 μL) contained 50 mM potassium phosphate buffer, at pH 7.0, 150×10^{-3} mM NADPH, 5×10^{-3} mM thioredoxin, $1{,}6 \times 10^{-3}$ mM thioredoxin reductase and different aliquots of crude extract, protein fractions, and Vu-2-Cys-Prx. NADPH oxidation was monitored as the decrease in A_{340} nm and one unit of activity (U) represents the change of one unit of absorbance within 1 min of reaction.
[b] Chitin-bound proteins eluted with 100 mM acetic acid.
[c] RQIV (Vu-2-Cys-Prx), protein eluted from the ion-exchange Resource Q® column with 300 mM NaCl in 50 mM sodium acetate buffer at pH 5.2.

3.2. Optimal pH of activity

Vu-2-Cys-Prx reduces H_2O_2 in the presence of the thiol-reducing systems thioredoxin and thioredoxin reductase at the expense of NADPH, as reported for the recombinant 2-Cys-Prx of Chinese cabbage (*B. campestris* L. ssp. *pekinensis*) [26]. The reaction kinetics showed a

gradual oxidation of NADPH from 0 up to 200 s of reaction (Fig. 3A). In addition, Vu-2-Cys-Prx reduced H_2O_2 using the reducing power of DTT *in vitro* (Fig. 3B). This observation suggests that DTT can directly reduce the intermolecular disulfide bonds at the end of the catalytic cycle by regenerating the free thiol forms of S_P and the S_R, the sulfur atoms of the peroxidatic and resolving cysteines, respectively, which are typically restored by a thioredoxin-like molecule [16].

Vu-2-Cys-Prx showed optimal activity at pH 7.0 regardless of the buffer used (Fig. 3C). However, for other pHs away from pH 7.0 the effect of the buffer was noted as statistic differences ($p \leq 0.05$) were found. 2-Cys-Prx from *Thunnus maccoyii* and *Taiwanofungus camphorata* have optimal activity at pH 7.0 and pH 8.0, respectively [52,53]. Higher or lower pHs led to the loss of peroxidatic activity of Vu-2-Cys-Prx (Fig. 3C) probably due to structural changes [54].

3.3. Oxidative states and pI of Vu-2-Cys-Prx

Two-dimensional electrophoresis (2D) analysis of Vu-2-Cys-Prx in the absence of β-mercaptoethanol gave two well-defined spots with unique molecular masses of approximately 42 kDa and pIs of 4.72 and 4.68, respectively, representing dimers of Vu-2-Cys-Prx in the oxidant and reduced forms (Fig. 4A). In the presence of β-mercaptoethanol, these spots assumed a molecular mass of approximately 22 kDa and pIs of 4.70 and 4.66, respectively (Fig. 4B), representing the different states of oxidation of the enzyme monomers. These acidic pIs of Vu-2-Cys-Prx are similar to the pIs of the 2-Cys-Prxs from *A. thaliana* (pIs = 4.91, 4.71) [8]. Under overoxidation conditions, the cysteine residues of *P. sativum* 2-Cys-Prx can be oxidized to sulfenic acid, producing changes in pI that can be detected by 2D [11]. This change in the redox status verified by the presence of different protein spots might represent the capacity of Vu-2-Cys-Prx to function as a redox switch, intracellularly reducing or regulating the presence of hydroperoxides. This capability is ensured by the presence of auxiliary enzymes such as thioredoxin, glutathione reductase and cyclophilin systems [18,25,19] and the more recently-described sulfiredoxin system [21].

The protein spots revealed by 2D were also identified by ESI-Q-TOF-MS/MS. The peptide masses determined were analyzed against relevant databases and were searched at NCBI. Subsequently, the

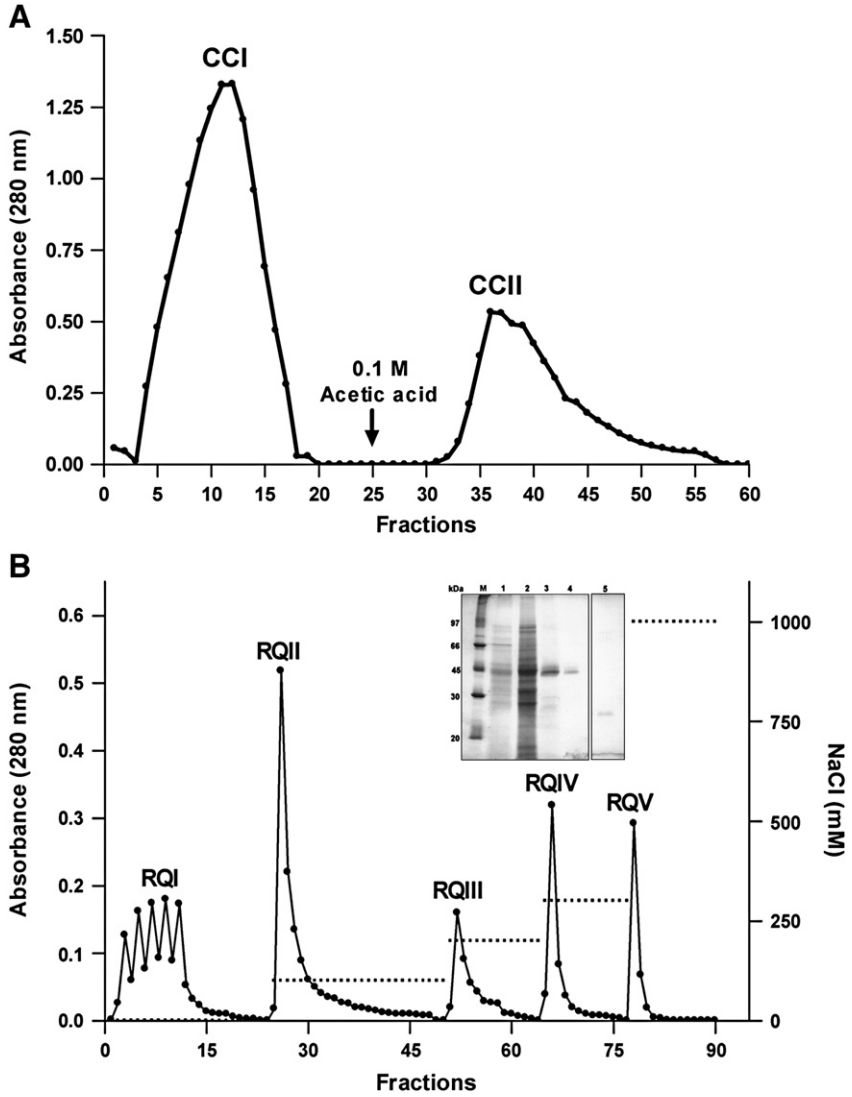

Fig. 1. Purification of Vu-2-Cys-Prx. (A) Affinity chromatography on a chitin column (197.8 mL). The fraction at 30–60% (F30–60) was applied to the column equilibrated with 50 mM sodium acetate buffer at pH 5.2 containing 0.5 M NaCl. The retained proteins (CCII), which contained 2-Cys-Prx activity, were eluted with 0.1 M acetic acid, and 3 mL fractions were collected at a 60 mL h^{-1} flow rate. (B) Ion exchange chromatography on Resource Q column (1.0 mL) equilibrated with 0.05 M sodium acetate buffer at pH 5.2. CCII was applied to the column (five injections), and the retained proteins were eluted with 0.1, 0.2, 0.3 and 1.0 M NaCl in the acetate buffer. Fractions (2.0 mL) were collected at a flow rate of 60 mL h^{-1} and were monitored for protein content at 280 nm. RQIV represents the purified Vu-2-Cys-Prx. Inset: Denaturing polyacrylamide gel electrophoresis (SDS-PAGE). M: molecular mass standards; Lane 1: cowpea leaf protein extract; lane 2: fraction at 30–60% ammonium sulfate saturation; lane 3: CCII; lane 4: purified Vu-2-Cys-Prx; lane 5: purified Vu-2-Cys-Prx in the presence of 5% β-mercaptoethanol.

peptide fragments of Vu-2-Cys-Prx generated by tryptic digestion were subjected to sequencing by MS/MS. The results of representative peptide spectra submitted to BLAST (NCBI) confirmed the identity of Vu-2-Cys-Prx as a typical 2-Cys-Prx. An excellent matching probability score of 94 ($P<0.05$) was obtained with sequence similar to the recombinant 2-Cys-Prx from *P. vulgaris* (CAC17803.1) [25].

3.4. NH_2-terminal sequence

Edman degradation of Vu-2-Cys-Prx provided 53 amino acid residues at the NH_2-terminal sequence: ASEELPLVGNIAPDFEAEAVFDQE FIKVKLSDYIGKKYVILFF YPLDFTFVCP (GenBank: AEA76433.1). Comparison of Vu-2-Cys-Prx with other known sequences showed a high sequence similarity with the recombinant 2-Cys-Prxs of *P. vulgaris* (CAC17803.1) (96%), *Populus thicocarpa* (EEF05155.1) (96%) and *P. sativum* (CAC48323.1) (94%). Furthermore, it showed that the primary structure of Vu-2-Cys-Prx has common features with the above recombinant 2-Cys-Prxs because there is a conserved cysteine residue at position 52 and an NH_2-terminal motif (LFFYPLDFTFVCP) highly conserved around the catalytic site. Other features were the presence of several hydrophobic amino acids, including seven phenylalanine residues (Phe^{16}, Phe^{22}, Phe^{26}, Phe^{42}, Phe^{43}, Phe^{48} and Phe^{50}) near the active site and two conserved amino acid residues (Pro^{45} and Thr^{49}) involved in the region of the active site [9,5,53]. To the best of our knowledge, only two leaf 2-Cys-Prx have been purified to homogeneity, i.e. from *Brassica napus* and that of *V. unguiculata* (Vu-2-Cys-Prx) here reported. On the basis of the Edman sequencing, it was unambiguously established that the N-terminal region of native rapeseed 2-Cys-Prx is AQADDLPLVG- [27]. This partial primary structure is identical to the two isoforms of Arabidopsis (species that also belongs to the *Brassicaceae* family), but it differs from those deduced for other species, mainly in the first five residues (Fig. 5). The alignment of the N-terminal amino acid sequences of Vu-2-Cys-Prx (Fig. 5) reveals that neither Ser^2 nor Glu^4 is strictly conserved, as suggested in Fig. 12 for putative sequences.

3.5. Structural results from spectroscopic measurements

The far-UV CD spectra of Vu-2-Cys-Prx at pH 7 showed minima at approximately 208 and 218 nm (Fig. 6), and deconvolution of the CD spectra performed using the CDPro package [38] and a reference set of 43 proteins revealed the following content of the secondary

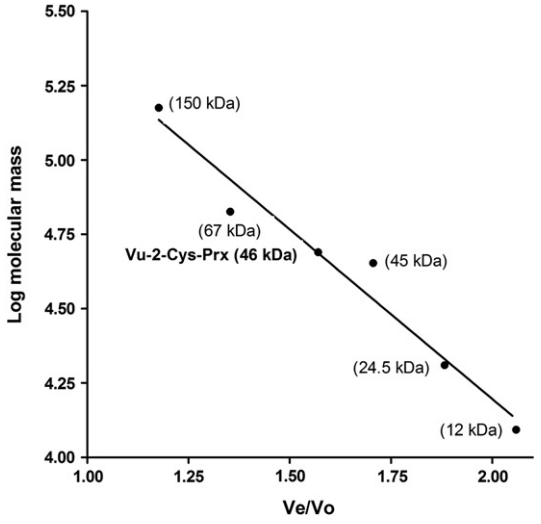

Fig. 2. Molecular mass determination of Vu-2-Cys-Prx by exclusion chromatography on Superose 12 HR. Protein samples were injected in the system and the elution profiles were monitored at 280 nm with a flow rate of 0.3 mL min^{-1}. Calibration was performed with alcohol dehydrogenase (150 kDa), BSA (66 kDa), egg albumin (45 kDa), trypsinogen (24.5 kDa), and cytochrome C (12 kDa).

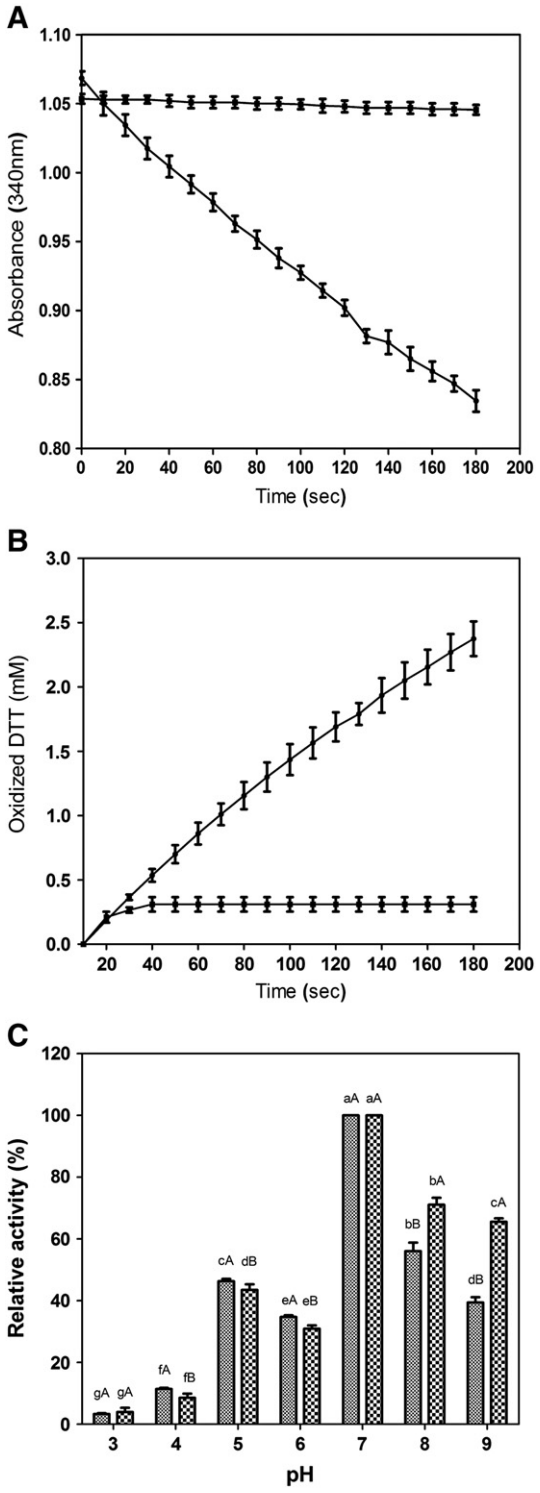

Fig. 3. Enzymatic activity of Vu-2-Cys-Prx in the presence of NADPH and DTT as reducing agents. (A) Reduction of H_2O_2 in the presence of thioredoxin and thioredoxin reductase with concomitant oxidation of NADPH in 50 mM sodium phosphate buffer pH 7.0. The reaction was performed at 30 °C for 200 s. (B) DTT oxidation in the presence (●) and absence (■) of Vu-2-Cys-Prx. Reaction mixture contained 150×10^{-3} mM H_2O_2, 1 mM EDTA and 50 mM sodium phosphate buffer pH 7.0. (C) Effect of pH on Vu-2-Cys-Prx activity. Reaction mixture was as described in (A). The following buffers were used for each pH assayed: pH 3.0, 50 mM sodium citrate and 50 mM glycine-HCl; pH 4.0 and 5.0, 50 mM sodium acetate and 50 mM sodium citrate; pH 6.0, 50 mM sodium acetate and 50 mM sodium phosphate; pH 7.0 and 8.0, 50 mM sodium phosphate and 50 mM Tris–HCl; pH 9.0, 50 mM Tris–HCl and 50 mM sodium borate. Different capital letters within the same pH value denote statistical difference at $p\leq0.05$. Different small letters between distinct pH values denote statistical difference at $p\leq0.05$.

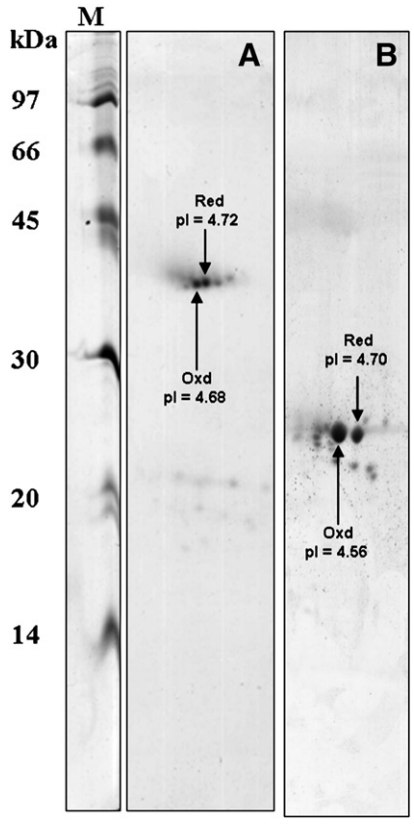

Fig. 4. Oxidation states and isoelectric point (pI) of Vu-2-Cys-Prx. Vu-2-Cys-Prx (6 μg) were focused on 11 cm IPG strips (pH 4–7) in the absence (A) and presence (B) of β-mercaptoethanol. After focusing, samples were subjected to two-dimensional gel electrophoresis, as described in the Materials and methods section. Protein spots were stained with colloidal Coomassie G-250. Oxd and Red represent oxidized and reduced states, respectively. (M) Molecular weight markers.

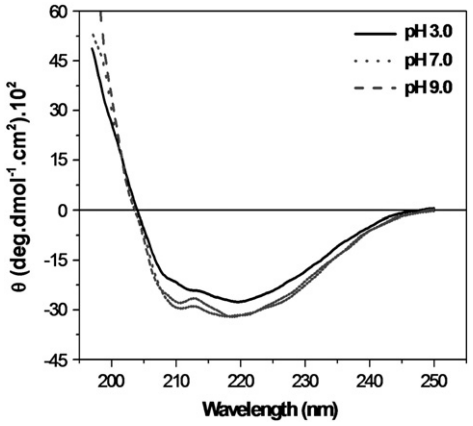

Fig. 6. Effect of pH on Vu-2-Cys-Prx conformation measured by circular dichroism spectra in 25 mM Glycine-HCl, pH 3, and 25 mM Tris–HCl, pH 7 and 9.0, using a 0.1 cm pathlength cylindrical quartz cuvette. Vu-2-Cys-Prx concentration was 90×10^{-3} mM.

structure fraction: 8% α-helix, 39% β-sheet, 22% turns and 31% unordered forms (RMSD 1%). Therefore, Vu-2-Cys-Prx can be classified as a *βII* class protein with respect to its CD spectral shape [55,56]. No significant changes in the CD spectra of Vu-2-Cys-Prx were observed after heat treatment up to 75 °C (Fig. 7A). At higher temperatures, typical conformational changes were observed, which were characteristic of denatured proteins because they were associated with the progressive loss of enzyme activity. *Saccharomyces cerevisiae* Prxs I and II did not modify their enzyme activity after heat treatment at 70 °C [41], but heat treatment at 60 °C of 2-Cys-Prxs from the medicinal mushroom *T. camphorata* decreased the enzyme activity by 40% [53]. Nevertheless, Vu-2-Cys-Prx can be regarded as a thermo-stable protein with an average melting temperature (Tm) of 74 °C, at which the native and denatured states are equally populated at equilibrium (Fig. 7B), suggesting a two-state model for thermal denaturation. Despite the relative thermal stability, Vu-2-Cys-Prx was unable to refold to its native structure after heating at 95 °C and cooling to 25 °C (Fig. 8). Additionally, the CD spectral shape did not change in the pH range from 3.0 to 9.0 and had a discrete alteration at pH 3.0 (Fig. 6).

The fluorescence emission of the intrinsic probe revealed that Vu-2-Cys-Prx showed no alteration in the emission maximum ($\lambda_{max} \approx 335$ nm) at pH 3, 7 and 9 (Figure not shown). Similar intrinsic fluorescence studies previously carried out with 2-Cys-Prx from barley showed similar $\lambda_{max} \approx 327$ nm [9]. Using ANS as extrinsic probe, the fluorescence emission spectra, in agreement with the CD

```
Vigna unguiculata                  -ASEELPLVGNIAPDFEAEAVFDQEFIKVKLSDYIGKKYVILFFYPLDFT 49
Brassica napus                     AQADDLPLVGNKAPDFEAEAVFDQEFIKVKLSEYIGKKYVLLFLYPLDFT 50
Arabidopsis thaliana 2-Cys-PrxA    AQADDLPLVGNKAPDFEAEAVFDQEFIKVKLSDYIGKKYVLLFFYPLDFT 50
Arabidopsis thaliana 2-Cys-PrxB    AQADDLPLVGNKAPDFEAEAVFDQEFIKVKLSEYIGKKYVLLFFYPLDFT 50
Populus trichocarpa                -ASSELPLVGNVAPDFEAEAVFDQEFIKVKLSEYIGNKYVVLFFYPLDFT 49
Triticum aestivum                  AAEYDLPLVGNKAPDFAAEAVFDQEFINVKLSDYIGKKYVLLFFYPLDFT 50
Secale cereale                     AAEYDLPLVGNKAPDFAAEAVFDQEFINVKLSDYIGKKYVLLFFYPLDFT 50
Hordeum vulgare                    AAEYDLPLVGNKAPDFAAEAVFDQEFINVKLSDYIGKKYVLLFFYPLDFT 50
Oryza sativa                       GGVDDAPLVGNKAPDFDAEAVFDQEFINVKLSDYIGKKYVLLFFYPLDFT 50
                                                                                  ******

Vigna unguiculata                  FVCP---------------------------------------------- 53
Brassica napus                     FVCPTEITAFSDRYEEFEKLNTEVLGVSVDSVFSHLAWVQTERKSGGLGD 100
Arabidopsis thaliana 2-Cys-PrxA    FVCPTEITAFSDRYEEFEKLNTEVLGVSVDSVFSHLAWVQTDRKSGGLGD 100
Arabidopsis thaliana 2-Cys-PrxB    FVCPTEITAFSDRHSEFEKLNTEVLGVSVDSVFSHLAWVQTDRKSGGLGD 100
Populus trichocarpa                FVCPTEITAFSDRYEEFKQINTEVLGVSVDSVFSHLAWVQTDRKSGGLGD 99
Triticum aestivum                  FVCPTEITAFSDRHEEFEKINTEILGVSVDSVFSHLAWVQTERKSGGLGD 100
Secale cereale                     FVCPTEITAFSDRHEEFEKINTEILGVSVDSVFSHLAWVQTERKSGGLGD 100
Hordeum vulgare                    FVCPTEITAFSDRHEEFEKINTEILGVSVDSVFSHLAWVQTERKSGGLGD 100
Oryza sativa                       FVCPTEITAFSDRYDEFEKLNTEILGVSIDSVFSHLAWVQTDRKSGGLGD 100
                                   ****
```

Fig. 5. Alignment of the N-terminal sequence of 2-Cys-Prx from *Vigna unguiculata* (Vu-2-Cys-Prx) with other 2-Cys-Prxs from plant species. The accession numbers of the sequences were *Brassica napus* (AAG30570.1), *Arabidopsis thaliana* 2-Cys-PrxA (Q96291.2), *Arabidopsis thaliana* 2-Cys-PrxB (Q9C5R8.3), *Populus trichocarpa* (XP_002309395.1), *T. aestivum* (P80602.2), *Secale cereale* (gb|AAC78473.1), *H. vulgare* (BAJ98505.1), and *Oryza sativa* (EEC73346.1). The alignment was generated using ClustalW program. Positions with conserved residues at the N-terminus and at the catalytic domain (box) are shaded in black whereas those containing conservative substitutions are shaded in gray. The conserved motif characteristic of typical 2-Cys-Prxs are boxed and indicated by asterisks (*).

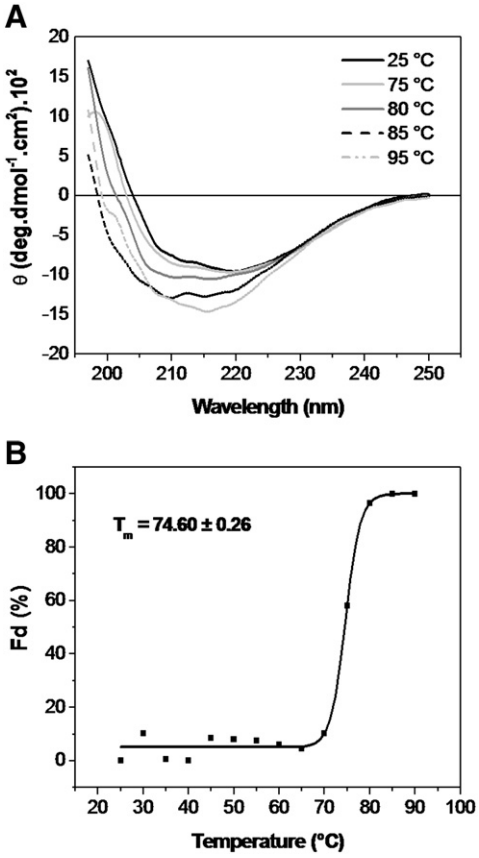

Fig. 7. (A) Effect of temperature on the CD spectra of Vu-2-Cys-Prx. Spectra were measured using a protein concentration of 90×10^{-3} mM in 25 mM Tris–HCl at pH 7.0 in a 0.1 cm pathlength cylindrical quartz cuvette. (B) Thermal denaturing curve of Vu-2-Cys-Prx plotted using CD values of the 202 nm bands as a function of temperature. Tm represent the melting temperature midpoint of 74.6 °C measured as the change of denatured Vu-2-Cys-Prx (Fd%) with increasing temperature.

data, showed no alteration in the emission maximum ($\lambda_{max}\approx515$ nm) at pH 7 (Fig. 9B) and pH 9 (Fig. 9C), which is very close to that for rapeseed 2-Cys-Prx ($\lambda_{max}\approx512$) at pH 7.0 [57]. However, at pH 3 (Fig. 9A), the emission fluorescence spectra from 380 to 650 nm of ANS coupled to Vu-2-Cys-Prx, showed a blue shift ($\lambda_{max}\approx475$ nm) as a result of structural modification with the exposition of hydrophobic domains where the ANS is bound. Thus, through this experimental

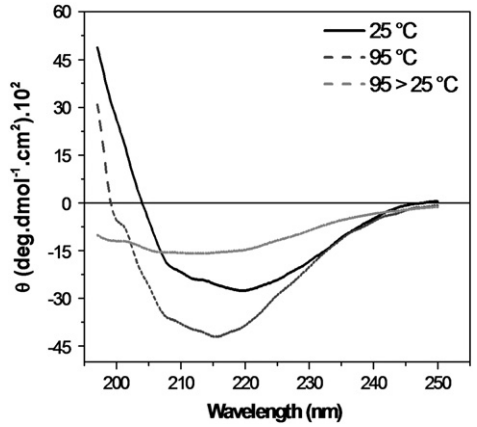

Fig. 8. Circular dichroism spectra of Vu-2-Cys-Prx after incubation at 25 °C, heating at 95 °C for 10 min, and heating at 95 °C for 10 min followed by incubation at 25 °C for 30 min. Spectra were measured using a protein concentration of 90×10^{-3} mM in 25 mM Tris–HCl, pH 7.0, in a 0.1 cm pathlength cylindrical quartz cuvette.

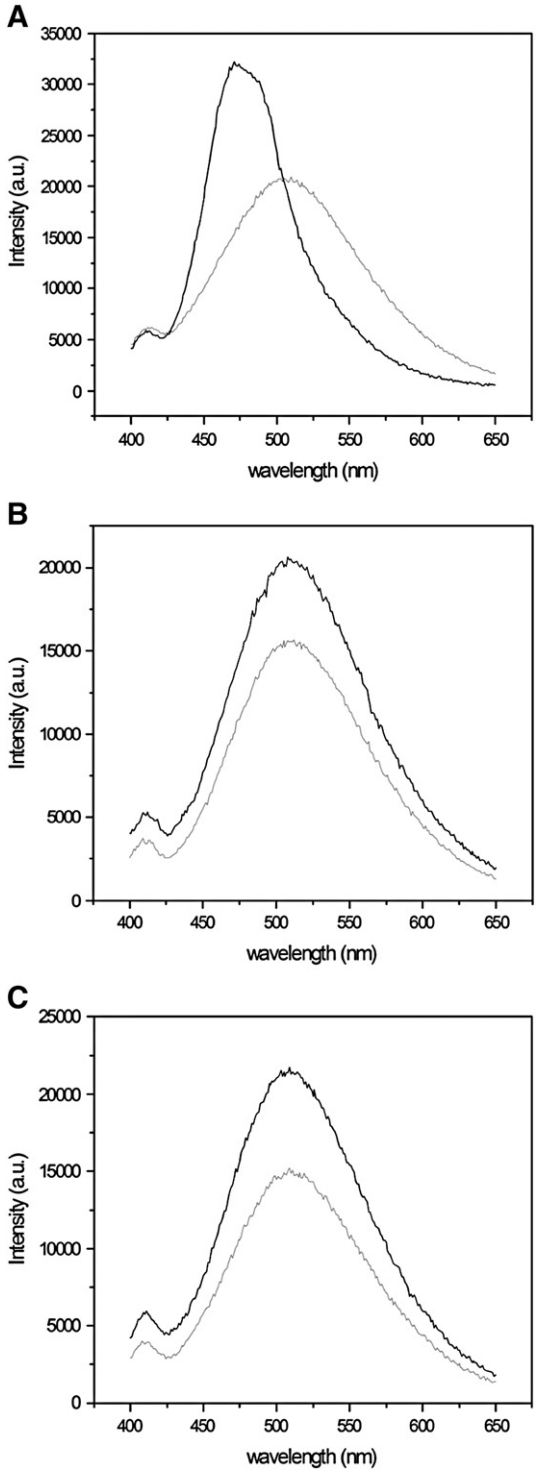

Fig. 9. Changes in surface hydrophobicity as a function of pH. Fluorescence emission spectra of 13.4 μM bis-ANS (gray) and bis-ANS bound to 90×10^{-3} mM of Vu-2-Cys-Prx (black line) in 25 mM glycine-HCl at pH 3 (A), 25 mM PBE at pH 7 (B) and Tris–HCl at pH 9.0 (C). Vu-2-Cys-Prx was excited at A_{380} nm.

approach, it was possible to verify structural alterations of Vu-2-Cys-Prx exposed to pH 3.0, which is in agreement with the loss of activity of the purified protein under low hydrogen ionic concentrations (Fig. 3C). Alternatively, the lack of alteration of λ_{max} at pH 9 (Fig. 9C) was not associated somehow with the functional stability of Vu-2-Cys-Prx because, at this pH, the ability of Vu-2-Cys-Prx to oxidize NADPH was not completely lost (Fig. 3C). Analysis of the putative amino acid sequence of Vu-2-Cys-Prx (Fig. 10) deduced from the

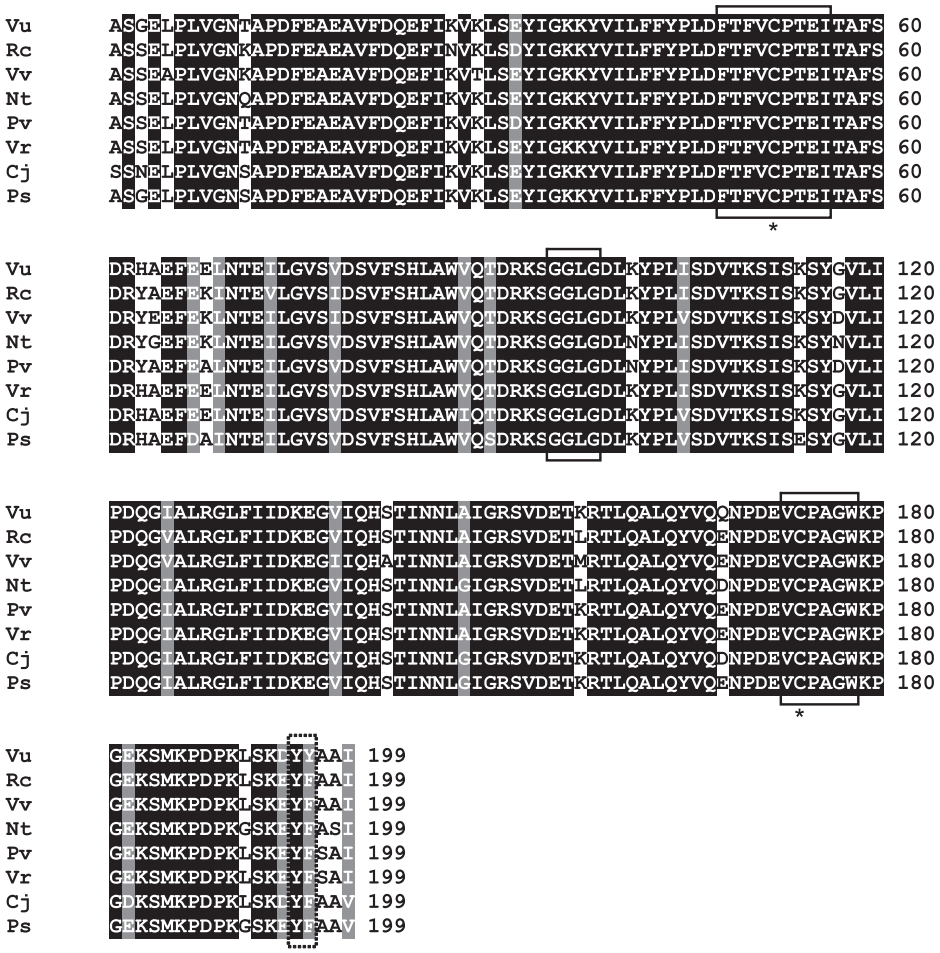

Fig. 10. Alignment of the amino acid sequence of Vu-2-Cys-Prx (this work) with representative sequences of typical 2-Cys-Prxs from other plant species. The amino acid sequences (retrieved from GenBank) aligned to the *Vu*-2-Cys-Prx primary structure are from *Ricinus cummunis* (Rc; accession number XP_002530152), *Vitis vinifera* (Vv; XP_002280930), *Nicotiana tabacum* (Nt; CAC84143), *P. vulgaris* (Pv; CAC17803), *Vigna radiata* (Vr; ACZ56426), *Caragana jubata* (Cj; ADX30686), and *Pisum sativum* (Ps; CAC48323). The alignment was generated using ClustalW program and shaded using Boxshade software (available at the web server www.ch.embnet.org/software/BOX_form.html). Positions with conserved residues are shaded in black whereas those containing conservative substitutions are shaded in gray. The conserved motifs characteristic of typical 2-Cys-Prxs are boxed and the two conserved cysteine residues are indicated by asterisks (*). The motif whose consensus sequence is YF is boxed with a dashed line.

corresponding cDNA obtained from cowpea leaf showed the presence of two tryptophan (Trp^{87} and Trp^{178}) residues, one of which (Trp^{178}) was very close to Cys^{174}.

3.6. Structural patterns of Vu-2-Cys-Prx

Vu-2-Cys-Prx behaved as homodimers in the presence of 100 mM H_2O_2, 1.5×10^3 mM NaCl, 50 mM Na-citrate buffer (pH 2.0), and 50 mM Na-borate buffer (pH 11.0) and when heated at 99 °C for 10 min. However, some of the Vu-2-Cys-Prx homodimers dissociated into monomers and assembled to form oligomers after treatment with 100 mM DTT as seen SDS-PAGE (Fig. 11A). By AFM, after treatment of Vu-2-Cys-Prx with 100 mM DTT and adsorption to a mica surface thousands of decameric Vu-2-Cys-Prx on a flat surface were observed (Fig. 12A). Moreover, a more detailed analysis (Fig. 12 B) revealed the presence of individual decamers, each with a central channel. A much high-resolution image of a Vu-2-Cys-Prx decamer showed (Fig. 12 C) a toroidal structure with five dimeric units assembled in a 20 nm oligomer, with a central pore of about 6.5 nm, which is compatible with other chaperone proteins such as GroEL (15 nm oligomer) from *E. coli* [58]. Thus Vu-2-Cys-Prx has a behavior of typical 2-Cys-Prx because it can exist in different conformational states (monomers, dimers, decamers and oligomers) when exposed to stress conditions such as over-reduction or over-oxidation of the environment [26,54,59]. In this respect it is well established that Prxs form a ring-like decamer based in observations *in vitro* by transmission electron microscopy and X-ray crystallography [60].

Interestingly, oligomerization of 2-Cys-Prx leads to the loss of peroxidatic activity and the concomitant appearance of chaperone activity [26,41]. Molecular chaperone function of 2-Cys-Prx was first described for two yeast cytosolic 2-Cys-Prx, cPrx I and cPrx II [41], and later for *Helicobacter pylori* alkyl hydroperoxide reductase (AhpC) [61]. Chaperone activity was also confirmed for 2-Cys-Prx of *B. napus* [57], *Chinese cabbage* [26] and *A. thaliana* [62]. Vu-2-Cys-Prx acts as a molecular chaperone as it prevented the chemical aggregation of insulin induced by DTT (Fig. 13A) and also the thermal aggregation of CS induced by heating at 45 °C (Fig. 13B). In *Chinese cabbage* the conformational transition of C2C-Prx1 into a chaperone provided protection to macromolecules in chloroplasts from aggregation under stress conditions [26]. On the other hand, inhibition of insulin and CS aggregation were not observed when incubated in the presence of BSA. The capacity of these enzymes to alter their conformational structure in response to stress conditions is very interesting, but the precise mechanism that regulates this structural changes and function is still unclear.

3.7. Antioxidant activity of Vu-2-Cys-Prx

It has been suggested that one of the physiological functions of the 2-Cys-Prxs is to detoxify endogenous reactive oxygen species, particularly H_2O_2, generated during photosynthesis and environmental

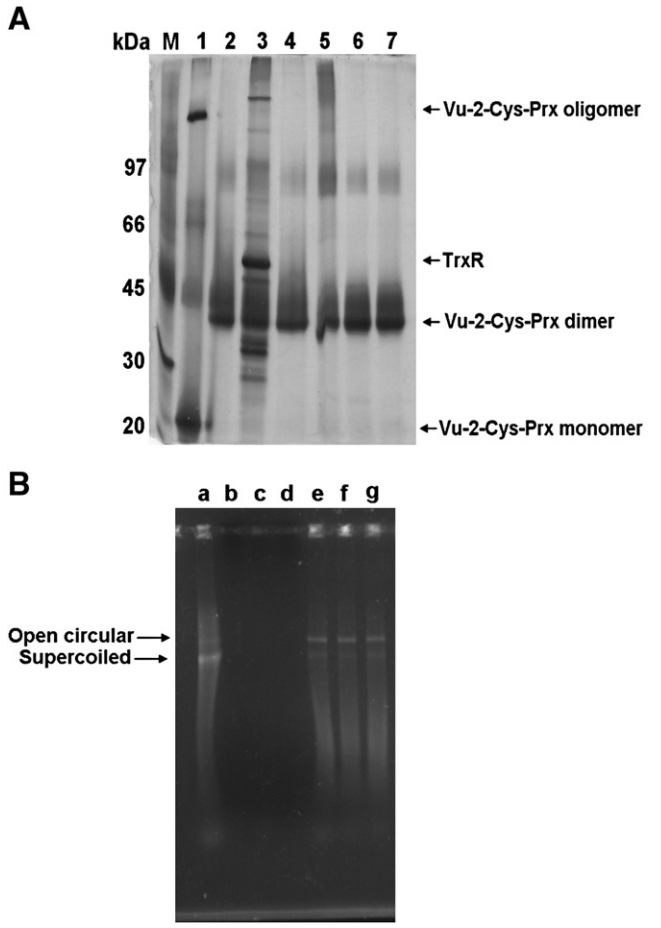

Fig. 11. (A) Oligomerization states of Vu-2-Cys-Prx. Vu-2-Cys-Prx was incubated in 50 mM of PBE buffer at pH 7.0 in different conditions: Lane 1, in the presence of 100 mM DTT; lane 2, untreated sample; lane 3, in the presence of 5×10^{-3} mM thioredoxin, 1.6×10^{-3} mM thioredoxin reductase, 150×10^{-3} mM NADPH and 100 mM H_2O_2; lane 4, in the presence of 1.5 M NaCl; lane 5, heated at 98 °C for 30 min; lanes 6 and 7, Vu-2-Cys-Prx dissolved in 50 mM Na-citrate buffer at pH 2.0, and 50 mM Na-borate buffer at pH 11.0, respectively. After every treatment, Vu-2-Cys-Prx (6 μg) was subjected to denaturing electrophoresis on a 12.5% gel, and protein bands were visualized with silver staining. (B) Protection of plasmid DNA from oxidation by the presence of Vu-2-Cys-Prx. Lane a, plasmid DNA; lanes b–d, plasmid DNA + 3×10^{-3} mM $FeCl_3$ + 10 mM DTT and bovine serum albumin at 23×10^{-6} mM (b), 45×10^{-6} mM (c) and 90×10^{-6} mM (d), respectively; lanes e–g, plasmid DNA + 3×10^{-3} mM $FeCl_3$ + 10 mM DTT + Vu-2-Cys-Prx at 23×10^{-3} mM (e), 45×10^{-3} mM (f) and 90×10^{-3} mM (g), respectively. After treatment, plasmid DNA was analyzed on ethidium bromide-stained 1% agarose gels.

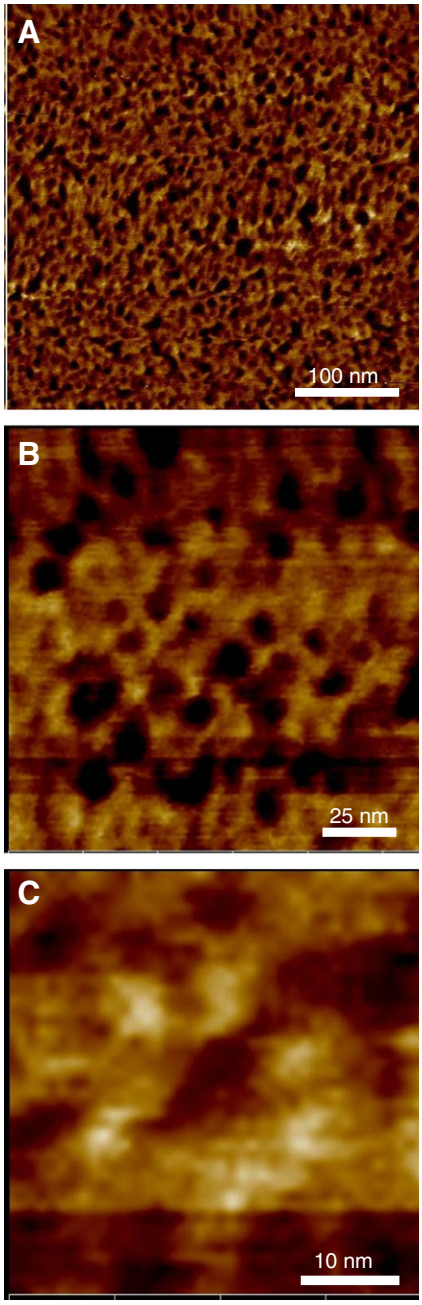

Fig. 12. Oligomerization analysis of Vu-2-Cys-Prx by atomic force microscopy (AFM) after treatment with 100 mM DTT. The high-resolution images were obtained by adsorption of Vu-2-Cys-prx surface on mica treated with poly-L-lysine. (A) Decameric structure of Vu-2-Cys-Prx on a flat mica surface. (B) Decameric structure of Vu-2-Cys-Prx showing a central channel characteristic of toroidal structure. (C) Detail of an individual decameric structure of Vu-2-Cys-Prx with the central channel (black) and its five constituent dimeric units.

stresses [19,22]. The *in vitro* activity of Vu-2-Cys-Prx against DNA oxidation by hydroxyl radicals formed by the Fenton reaction between DTT and $FeCl_3$ [40] was thus assessed. The results showed that when the plasmid DNA from pGEM T-easy obtained commercially was incubated in the absence of $FeCl_3$ and DTT, open circular and coiled DNA were observed (Fig. 11B) after electrophoresis on agarose gel. However, incubation with $FeCl_3$, DTT and BSA promoted the complete degradation of the plasmid DNA after 3 h at 37 °C. In contrast, substitution of BSA for Vu-2-Cys-Prx in the reaction mixture containing $FeCl_3$, and DTT protected the plasmid DNA from oxidative damage and degradation, showing the antioxidant activity of Vu-2-Cys-Prx. Similar results were obtained for a barley 2-Cys-Prx and for 2-Cys-Prxs from *Chinese cabbage* (C2C-Prx), *P. vulgaris* (*PvPrx*) and from *P. sativum* (PsPrx II) [63,40,25,19,59].

3.8. Cloning and sequence analysis

A partial cDNA sequence (597 bp) encoding the mature form (199 amino acid residues) of Vu-2-Cys-Prx was amplified by RT-PCR from leaves of 15-day-old cowpea plants (Fig. 10). The encoded polypeptide had a predicted molecular mass of 22,111.16 Da and a theoretical pI of 4.7. When the N-terminal sequence (53 residues) determined by Edman degradation from the protein purified from cowpea leaves (as already described) was compared with the amino acid sequence deduced from the cDNA, an almost identical match was found, except for two residues. In the cDNA encoded sequence, Gly^3 and Glu^{32} are replaced by Glu and Asp, respectively, in the sequence of the protein purified from leaves. Therefore, the cDNA encodes a 2-Cys-Prx isoform closely related to the protein purified to homogeneity from the same tissue. Searches on the GenBank protein database revealed high identity scores (94–98%) between *V. unguiculata* 2-Cys-Prx

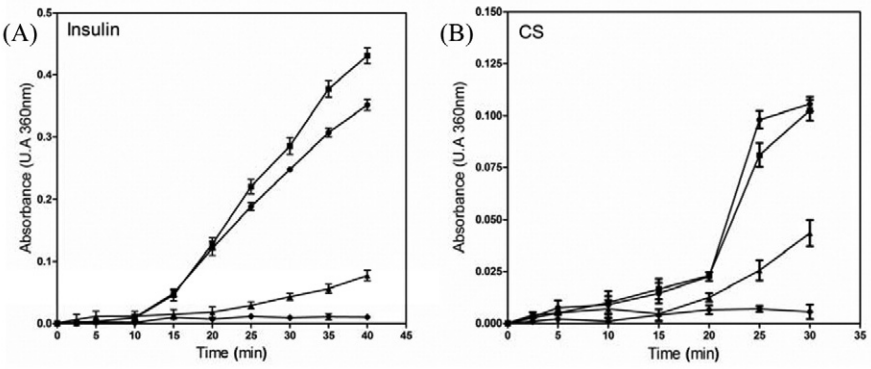

Fig. 13. Molecular chaperone activity of Vu-2-Cys-Prx (10^{-3} mM) on insulin and citrate synthase (CS). The chaperone function was measured as a function of the chemical aggregation of insulin (A) and thermal aggregation of CS (B) induced by 10 mM DTT and incubation at 45 °C, respectively. Insulin and CS in the presence of Vu-2-Cys-Prx (▲). BSA (5×10^{-3} mM) (●) was used as control in the presence of insulin and CS, BSA in the absence of insulin and CS (■), Vu-2-Cys-Prx in the absence of insulin and CS (♦). Protein aggregation was monitored by measuring the absorbance at $A_{360\ nm}$.

sequence (cDNA encoded) and homologous protein sequences from other Fabaceae species, such as *Vigna radiata* (98%), *Caragana jubata* (95%), *P. vulgaris* (95%) and *P. sativum* (94%). A high sequence identity was also evident between Vu-2-Cys-Prx and 2-Cys-Prxs from species belonging to other plant families such as *Populus trichocarpa* (Salicaceae; 94%), *Ricinus cumunnis* (Euphorbiaceae; 93%) and *Vitis vinifera* (Vitaceae; 92%). The multiple alignment of these plant 2-Cys-Prxs showed that a high proportion of their amino acid residues (83.4%; 166 out of 199) are conserved. The conserved regions included the motifs ^{48}FTFVCPTEI^{56}, containing the peroxidatic Cys residue (Cys^{52}), and the hydrophobic segment ^{173}VCPAGW^{178}, containing the resolving Cys residue (Cys^{174}), as highlighted in (Fig. 10). These two motifs, particularly the Cys residues, are distinctive features shared by typical 2-Cys-Prx that occur in all kingdoms of life [64,9]. The Cys^{52} residue together with Thr^{49} and Arg^{128} (both of which are also conserved in Vu-2-Cys Prx) constitutes the catalytic triad of typical 2-Cys-Prxs. In this catalytic mechanism, deprotonation of the solvent-exposed thiol of Cys^{52} is facilitated by hydrogen bonding with the threonine hydroxyl group and the positive charge of the arginine side chain [65,54]. A third conserved motif, ^{95}GGLG^{98}, is also present in the Vu-2-Cys-Prx sequence. This motif is common in most typical eukaryotic 2-Cys-Prxs but is absent from most prokaryotic typical 2-Cys-Prxs [64]. In eukaryotes, the GGLG motif is associated with the YF (Tyr-Phe) motif, and these two motifs have been proposed as the structural origin of the sensitivity to overoxidation observed in eukaryotic typical 2-Cys-Prxs [64]. Interestingly, in the Vu-2-Cys-Prx sequence, the phenylalanine residue is replaced by tyrosine (^{195}YY^{196} instead of YF). However, this conservative substitution (both Y and F have aromatic side chains) may have little effect on the enzymatic properties of Vu-2-Cys-Prx. Moreover, the typical 2-Cys-prxs are obligate homodimers, which, in turn, oligomerize into stable decamers (pentamers of dimers) [64]. Searches on the Conserved Domain Database (CDD) allowed mapping of Vu-2-Cys-Prx residues predicted to be located at the monomer–monomer interface (Val^{8}, Phe^{50}, Val^{51}, Thr^{54}, Gly^{117}, Leu^{127}, Gln^{140}–Ser^{142}, Ile^{144}–Asn^{146}, Gly^{150}, Arg^{151}, Arg^{158}, and Cys^{174}–Gly^{177}) in the dimers. Besides, the Vu-2-Cys-Prx residues predicted to be located at the dimer-dimer interface (Phe^{48}, Phe^{82}, Ser^{83}, Val^{108}, Lys^{110}, and Asp^{122}) in the decameric structure were also mapped. Thus, this comparative sequence analysis shows clearly that the cloned cDNA from *V. unguiculata* encodes a typical 2-Cys-Prx.

4. Conclusion

Vu-2-Cys-Prx represents the second 2-Cys-Prx that has been purified to homogeneity. The novelty of this work lies mainly in the finding that Vu-2-Cys-Prx contains a motif that binds to chitin, which opens the possibility that this protein could act against some plant plagues and pests in addition to its function as a peroxidase and molecular chaperone. For example, a Prx from poplar (PrxII F) was upregulated during compatible fungal interaction and was downregulated during incompatible pathogen-poplar interaction [20].

Acknowledgments

This work was supported by CNPq, CAPES and FUNCAP. Silva FDA was granted a M.Sc. fellowship from CAPES. We are grateful to UNIPROTE-MS (UFRGS-Brazil) for the spectrometric analysis.

References

[1] C. Lamb, R.A. Dixon, The oxidative burst in plant disease resistance, Annu. Rev. Plant Phys. Mol. Biol. 48 (1997) 251–275.
[2] K.E. Apel, H. Hirt, Reactive oxygen species: metabolism, oxidative stress, and signal transduction, Annu. Rev. Plant Biol. 55 (2004) 373–399.
[3] G. Miller, N. Suzuki, S.E. Ciftci-Yilmaz, R. Mittler, Reactive oxygen species homeostasis and signalling during drought and salinity stresses, Plant Cell Environ. 33 (2010) 453–467.
[4] J. Feierabend, Catalases in plants: molecular and functional properties and role in stress defence, in: N. Smirnoff (Ed.), Antioxidants and Reactive Oxygen Species in Plants, Blackwell Publishing, Oxford, 2005, pp. 101–140.
[5] K. Asada, The water–water cycle in chloroplast: scavenging of active oxygen's and dissipation excess photons, Annu. Rev. Plant Biol. 50 (1999) 601–639.
[6] K.J. Dietz, S. Jacob, M.L. Oelze, M. Laxa, V. Tognetti, S.M.N. de Miranda, M. Baier, I. Finkemeier, The function of peroxiredoxins in plant organelle redox metabolism, J. Exp. Bot. 57 (2006) 1697–1709.
[7] B. Knoops, E. Loumaye, V. van der Eecken, Evolution of the peroxiredoxins, in: L. Flohé, J.R. Harris (Eds.), Peroxiredoxin Systems, Springer, New York, 2007, pp. 27–40.
[8] K.J. Dietz, Plant peroxiredoxins, Annu. Rev. Mol. Biol. 54 (2003) 93–107.
[9] J. König, K. Lotte, R. Plessow, A. Brockhinke, M. Baier, K.J. Dietz, Reaction mechanism of plant 2-cys-peroxiredoxin, J. Biol. Chem. 278 (2003) 24409–24420.
[10] F. Horling, P. Lamkemeyer, J. König, I. Finkemeier, A. Kandlbinder, M. Baier, K.J. Dietz, Divergent light, ascorbate, and oxidative stress-dependent regulation of expression of the peroxiredoxin gene family in Arabidopsis, Plant Physiol. 131 (2003) 317–325.
[11] S. Barranco-Medina, T. Krell, I. Finkemeier, F. Sevilla, J.J. Lázaro, K.J. Dietz, Biochemical and molecular characterization of the mitochondrial peroxiredoxin PsPrxII F from *Pisum sativum*, Plant Physiol. Biochem. 45 (2007) 729–739.
[12] K.J. Dietz, F. Horling, J. König, M. Baier, The function of the chloroplast 2-cysteine peroxiredoxin in peroxide detoxification and its regulation, J. Exp. Bot. 53 (2002) 1321–1329.
[13] A. Sakamoto, S. Tsukamoto, H. Yamamoto, M. Ueda-Hashimoto, M. Takahashi, H. Suzuki, H. Morikawa, Functional complementation in yeast reveals a protective role of chloroplast 2-Cys-peroxiredoxin against reactive nitrogen species, Plant J. 33 (2003) 841–851.
[14] M.D. Kim, Y.H. Kim, S.Y. Kwon, B.Y. Jang, S.Y. Lee, S.S. Kwak, H.S. Lee, Overexpression of 2-cysteine peroxiredoxin enhances tolerance to methyl viologen-mediated oxidative stress and high temperature in potato plants, Plant Physiol. Biochem. 49 (2011) 891–897.

[15] H.H. Jang, Y.H. Chi, S.K. Park, S.S. Lee, J.R. Lee, J.H. Park, J.C. Moon, Y.M. Lee, S.Y. Kim, K.O. Lee, S.Y. Lee, Structural and functional regulation of eukaryotic 2-cys-peroxiredoxins including the plant ones in cellular defense signaling mechanisms against oxidative stress, Physiol. Plant. 126 (2006) 549–559.
[16] A. Hall, P.A. Karplus, L.B. Poole, Typical 2-Cys peroxiredoxins: structures, mechanisms and functions, FEBS J. 276 (2009) 2469–2477.
[17] P. Pulido, R. Cazalis, F.J. Cejudo, An antioxidant redox system in the nucleus of wheat seed cells suffering oxidative stress, Plant J. 57 (2009) 132–145.
[18] H.Z. Chae, S.W. Kang, S.G. Rhee, Isoforms of mammalian peroxiredoxins that reduce peroxides in presence of thioredoxin, Methods Enzymol. 300 (1999) 219–226.
[19] L. Bernier-Villamor, E. Navarro, F. Sevilla, J.J. Lázaro, Cloning and characterization of a 2-Cys peroxiredoxin from *Pisum sativum*, J. Exp. Bot. 55 (2004) 2191–2199.
[20] F. Gama, O. Keech, F. Eymery, I. Finkemeier, E. Gelhaye, P. Gardeström, K.J. Dietz, P. Rey, J.P. Jacquot, N. Rouhier, The mitochondrial type II peroxiredoxin from poplar, Physiol. Plant. 129 (2007) 196–206.
[21] I. Iglesias-Baena, S. Barranco-Medina, A. Lázaro-Payo, F.J. López-Jaramillo, F. Sevilla, J.J. Lázaro, Characterization of plant sulfiredoxin and role of sulphinic form of 2-Cys-peroxiredoxin, J. Exp. Bot. 61 (2010) 1509–1521.
[22] P. Pulido, M.C. Spínola, K. Kirchsteiger, M. Guinea, M.B. Pascual, M. Sahrawy, S.M. Sandalio, K.J. Dietz, M. González, F.J. Cejudo, Functional analysis of the pathways for 2-Cys-peroxiredoxin reduction in *Arabidopsis thaliana* chloroplasts, J. Exp. Bot. 61 (2010) 4043–4054.
[23] M.B. Pascual, A. Mata-Cabana, F.J. Florencio, M. Lindahl, C.J. Cejudo, A comparative analysis of the NADPH thioredoxin reductase C 2-Cys-peroxiredoxin system from plants and cyanobacteria, Plant Physiol. 155 (2011) 1806–1816.
[24] A. Tovar-Méndez, M.A. Matamoros, P. Bustos-Sanmamed, K.J. Dietz, F.J. Cejudo, N. Rouhier, S. Sato, T. Satoshi, M. Becana, Peroxiredoxins and NADPH-dependent thioredoxin systems in the model legume *Lotus japonicus*, Plant Physiol. 156 (2011) 1535–1547.
[25] G. Genot, H. Wintz, G. Hounlé, E. Jamet, Molecular characterization of a bean chloroplastic 2-Cys-peroxiredoxin, Plant Physiol. Biochem. 39 (2001) 449–459.
[26] S.Y. Kim, H.H. Jang, J.R. Lee, N.R. Sung, H.B. Lee, D.H. Lee, D.J. Park, C.H. Kang, W.S. Chung, C.O. Lim, D.J. Yun, W.Y. Kim, K.O. Lee, S.Y. Lee, Oligomerization and chaperone activity of a plant 2-Cys-peroxiredoxin in response to oxidative stress, Plant Sci. 177 (2009) 227–232.
[27] D. Caporaletti, A.C. D'Alessio, R.J. Rodriguez-Suarez, A.M. Senn, P.D. Duek, R.A. Wolosiuk, Non-reductive modulation of chloroplast fructose 1,6-bisphosphatase by 2-Cys-peroxiredoxin, Biochem. Biophys. Res. Commun. 355 (2007) 722–727.
[28] J.A.G. Silveira, R.C.L. Costa, J.T.A. Oliveira, Drought-induced effects and recovery of nitrate assimilation and nodule activity in cowpea plants inoculated with *Bradyrhizobium* spp. under moderate nitrate level, Braz. J. Microbiol. 32 (2001) 187–194.
[29] M.M. Bradford, A rapid and sensitive method for the quantitation of microgram quantities of protein utilizing the principle of protein-dye binding, Anal. Biochem. 72 (1976) 248–254.
[30] R. Chauhan, S.C. Mande, Site-directed mutagenesis reveals a novel catalytic mechanism of *Mycobacterium tuberculosis* alkylhydroperixidase C, Biochem. J. 367 (2002) 255–261.
[31] U.K. Laemmli, Cleavage of structural proteins during the assembly of the head of bacteriophage T4, Nature 227 (1970) 680–685.
[32] G. Candiano, M. Bruschi, L. Musante, L. Santucci, G.M. Ghiggeri, B. Carnemolla, P. Orecchia, L. Zardi, P.G. Righetti, Blue silver: a very sensitive colloidal coomassie G-250 staining for proteome analysis, Electrophoresis 25 (2004) 1327–1333.
[33] F.A.S. Silva, C.A.V. Azevedo, Principal Components Analysis in the Software Assistat-Statistical Attendance, World Congress on Computers in Agriculture, 7, American Society of Agricultural and Biological Engineers, Reno-NV-USA, 2009.
[34] T. Rabilloud, M. Chevallet, Solubilization of proteins in 2-D electrophoresis, in: T. Rabilloud (Ed.), Proteome Research: Two-dimensional Gel Electrophoresis and Identification Methods, Springer-Verlag, Heidelberg, 2000, pp. 9–30.
[35] A. Görg, C. Obermaier, G. Boguth, A. Harder, B. Scheibe, R. Wildgruber, W. Weiss, The current state of two-dimensional electrophoresis with immobilized pH gradients, Electrophoresis 21 (2000) 1037–1053.
[36] S.F. Altschul, W. Gish, W. Miller, E.W. Myers, D.J. Lipman, Basic local alignment search tool, J. Mol. Biol. 215 (1990) 403–410.
[37] A. Shevchenko, M. Wilm, O. Vorm, M. Mann, Mass spectrometric sequencing of proteins from silver-stained polyacrylamide gels, Anal. Chem. 68 (1996) 850–858.
[38] N. Sreerama, R.W. Woody, Estimation of protein secondary structure from circular dichroism spectra: comparison of CONTIN, SELCON, and CDSSTR methods with an expanded reference set, Anal. Biochem. 287 (2000) 252–260.
[39] G.V. Semisotnov, N.A. Rodionova, O.I. Razgulyaev, V.N. Uversky, A.F. Gripas, R.I. Gilmanshin, Study of the "molten globule" intermediate state in protein folding by a hydrophobic fluorescent probe, Biopolymers 31 (1991) 119–128.
[40] R.A.P. Stacy, E. Munthe, T. Steinum, B. Sharma, R.B. Aalen, A peroxiredoxin antioxidant is encoded by a dormancy-related gene *Per1*, expressed during late development in the aleurone and embryo of barley grains, Plant Mol. Biol. 31 (1996) 1205–1216.
[41] H.H. Jang, K.O. Lee, Y.H. Chi, B.G. Jung, S.K. Park, J.H. Park, J.R. Lee, S.S. Lee, J.C. Moon, J.W. Yun, Y.O. Choi, W.Y. Kim, J.S. Kang, G.W. Cheong, D.J. Yun, S.G. Rhee, M.J. Cho, S.Y. Lee, Two enzymes in one: two yeast peroxiredoxins display oxidative stress-dependent switching from a peroxidase to a molecular chaperone function, Cell 117 (2004) 625–635.
[42] J. Sambrook, E.F. Fritsch, T. Maniatis, Molecular Cloning: A Laboratory Manual, Cold Spring Harbor Laboratory Press, Cold Spring Harbor, New York, 1989.
[43] G. Vatcher, D. Smailus, M. Krzywinski, R. Guin, J. Stott, M. Tsai, S. Chan, P. Pandoh, G. Yang, J. Asano, T. Olson, A.L. Prabhu, R. Coope, A. Marziali, J. Schein, S. Jones, M. Marra, Resuspension of DNA sequencing reaction products in agarose increases sequence quality on an automated sequencer, Biotechniques 33 (2002) 532–538.
[44] E.C. Almira, N. Panayotova, W.G. Farmerie, Capillary DNA sequencing: maximizing the sequence output, J. Biomol. Tech. 14 (2003) 270–277.
[45] X. Huang, A. Madan, CAP3: a DNA sequence assembly program, Genome Res. 9 (1999) 868–877.
[46] J.D. Thompson, D.G. Higgins, T.J. Gibson, CLUSTAL W: improving the sensitivity of progressive multiple sequence alignment through sequence weighting, position-specific gap penalties and weight matrix choice, Nucleic Acids Res. 22 (1994) 4673–4680.
[47] T.A. Hall, BioEdit: a user-friendly biological sequence alignment editor and analysis program for Windows 95/98/NT, Nucleic Acids Symp. 41 (1999) 95–98.
[48] I.V. Maksimov, E.A. Cherepanova, O.I. Kuzmina, L.G. Yarullina, A.A. Akhunov, Molecular peculiarities of the chitin-binding peroxidases of plants, Russ. J. Bioorg. Chem. 36 (2010) 293–300.
[49] M.P. Sales, V.M. Gomes, K.V.S. Fernandes, J. Xavier-Filho, Chitin-binding proteins from cowpea (*Vigna unguiculata*) seeds, Braz. J. Med. Biol. Res. 29 (1996) 319–326.
[50] N. Rouhier, E. Gelhaye, J.M. Gualberto, M.N. Jordy, E. De Fay, M. Hirasawa, S. Duplessis, S.D. Lemaire, P. Frey, F. Martin, W. Manieri, D.B. Knaff, J.P. Jacquot, Poplar peroxiredoxin Q: a thioredoxin-linked chloroplast antioxidant functional in pathogen defense, Plant Physiol. 134 (2004) 1027–1038.
[51] H.Z. Chae, S.J. Chung, S.G. Rhee, Thioredoxin dependent peroxide reductase from yeast, J. Biol. Chem. 269 (1994) 27670–27678.
[52] D.L. Sutton, G.H. Loo, R.I. Menz, K.A. Schuller, Cloning and functional characterization of a typical 2-Cys peroxiredoxin from southern bluefin tuna (*Thunnus maccoyii*), Comp. Biochem. Physiol. B Biochem. Mol. Biol. 156 (2010) 97–106.
[53] Y.J. Liau, Y.T. Chen, C.Y. Lin, J.K. Huang, C.T. Lin, Characterization of 2-Cys peroxiredoxin isozyme (Prx1) from *Taiwanofungus camphorata*: Expression and enzyme properties, Food Chem. 119 (2010) 154–160.
[54] Z.A. Wood, E. Schröder, J. Robin Harris, L.B. Poole, Structure, mechanism and regulation of peroxiredoxins, Trends Biochem. Sci. 28 (2003) 32–40.
[55] N. Sreerama, R.W. Woody, Structural composition of ßI and ßII-proteins, Protein Sci. 12 (2003) 384–388.
[56] J. Wu, J.T. Yang, C.S.C. Wu, β-II conformation of all-β proteins can be distinguished from unordered form by circular dichroism, Anal. Biochem. 200 (1992) 359–364.
[57] M. Aran, D. Caporaletti, A.M. Senn, M.T. Tellez de Iñon, M.R. Girotti, A.S. Ilera, R.A. Wolosiuk, ATP-dependent modulation and autophosphorylation os rapeseed 2-Cys peroxiredoxina, FEBS J. 275 (2008) 1450–1463.
[58] J. Mou, S.J. Sheng, R. Ho, Z. Shao, Chaperonins GroEL and GroES: views from atomic force microscopy, Biophys. J. 71 (1996) 2213–2221.
[59] S. Barranco-Medina, J.J. Lázaro, K.J. Dietz, The oligomeric conformation of peroxiredoxins links redox state to function, FEBS Lett. 583 (2009) 1809–1816.
[60] J.R. Harris, E. Schröder, M.N. Isupov, D. Scheffler, P. Kristensen, J.A. Littlechild, A.A. Vagin, U. Meissner, Comparison of the decameric structure of peroxiredoxin-II by transmission electron microscopy and X-ray crystallography, Biochim. Biophys. Acta 1547 (2001) 221–234.
[61] M.H. Chuang, M.S. Wu, W.L. Lo, J.T. Lin, C.H. Wong, S.H. Chiou, The antioxidant protein alkylhydroperoxide reductase of *Helicobacter pylori* switches from a peroxide reductase to a molecular chaperone function, Proc. Natl. Acad. Sci. 103 (2006) 2552–2557.
[62] M. Muthuramalingam, T. Seidel, M. Laxa, S.M. Nunes de Miranda, F. Gärtner, E. Ströher, A. Kandlbinder, K.-J. Dietz, Multiple redox and non-redox interactions define 2-Cys peroxiredoxin as a regulatory hub in the chloroplast, Mol. Plant 2 (2009) 1273–1288.
[63] N.E. Cheong, O.K. Choi, K.O. Lee, W.Y. Kim, B.G. Jung, Y.H. Chi, J.S. Jeong, K. Kim, M.J. Cho, S.Y. Lee, Molecular cloning, expression, and functional characterization of a 2-Cys-peroxiredoxin in Chinese cabbage, Plant Mol. Biol. 40 (1999) 825–834.
[64] Z.A. Wood, L.B. Poole, P.A. Karplus, Peroxiredoxin evolution and the regulation of hydrogen peroxide signaling, Science 300 (2003) 650–653.
[65] L. Flohé, H. Budde, K. Bruns, H. Castro, J. Clos, B. Hofmann, S. Kansal-Kalavar, D. Krumme, U. Menge, K. Plank-Schumacher, H. Sztajer, J. Wissing, C. Wylegalla, H.J. Hecht, Tryparedoxin peroxidase of *Leishmania donovani*: molecular cloning, heterologous expression, specificity, and catalytic mechanism, Arch. Biochem. Biophys. 397 (2002) 324–335.